Neurotoxicology 75 (2019) 89–104

Contents lists available at ScienceDirect

Neurotoxicology

journal homepage: www.elsevier.com/locate/neuro

Full length article

Neuroprotective effects of glucomoringin-isothiocyanate against H_2O_2-Induced cytotoxicity in neuroblastoma (SH-SY5Y) cells

Mohammed Sani Jaafaru[a,b], Norshariza Nordin[c], Rozita Rosli[c,d], Khozirah Shaari[e,f], Hauwa'u Yakubu Bako[b], Norazalina Saad[d], Noramaliza Mohd Noor[g], Ahmad Faizal Abdull Razis[a,h,i,*]

[a] Laboratory of Molecular Biomedicine, Institute of Bioscience, Universiti Putra Malaysia, 43400, UPM Serdang, Selangor, Malaysia
[b] Department of Biochemistry, Kaduna State University, Main Campus, PMB 2339, Kaduna, Nigeria
[c] Department of Biomedical Sciences, Faculty of Medicine and Health Sciences, Universiti Putra Malaysia, 43400, UPM Serdang, Selangor, Malaysia
[d] UPM-MAKNA Cancer Research Laboratory, Institute of Bioscience, Universiti Putra Malaysia, 43400, UPM Serdang, Selangor, Malaysia
[e] Laboratory of Natural Products, Institute of Bioscience, Universiti Putra Malaysia, 43400, UPM Serdang, Selangor, Malaysia
[f] Department of Chemistry, Faculty of Science, Universiti Putra Malaysia, 43400, UPM Serdang, Selangor, Malaysia
[g] Department of Imaging, Faculty of Medicine and Health Sciences, Universiti Putra Malaysia, 43400, UPM Serdang, Selangor, Malaysia
[h] Department of Food Science, Faculty of Food Science and Technology, Universiti Putra Malaysia, 43400, UPM Serdang, Selangor, Malaysia
[i] Laboratory of Food Safety and Food Integrity, Institute of Tropical Agriculture and Food Security, Universiti Putra Malaysia, 43400, UPM Serdang, Selangor, Malaysia

ARTICLE INFO

Keywords:
Glucomoringin isothiocyanate
Neurodegeneration
Neuroprotection
Signalling pathways
Neuroblastoma
SH-SY5Y differentiation

ABSTRACT

Neurodegenerative diseases (NDDs) are pathological conditions characterised by progressive damage of neuronal cells leading to eventual loss of structure and function of the cells. Due to implication of multi-systemic complexities of signalling pathways in NDDs, the causes and preventive mechanisms are not clearly delineated. The study was designed to investigate the potential signalling pathways involved in neuroprotective activities of purely isolated glucomoringin isothiocyanate (GMG-ITC) against H_2O_2-induced cytotoxicity in neuroblastoma (SH-SY5Y) cells. GMG-ITC was isolated from *Moringa oleifera* seeds, and confirmed with NMR and LC-MS based methods. Gene expression analysis of phase II detoxifying markers revealed significant increase in the expression of all the genes involved, due to GMG-ITC pre-treatment. GMG-ITC also caused significant decreased in the expression of *NF-kB, BACE1, APP* and increased the expressions of *IkB* and *MAPT* tau genes in the differentiated cells as confirmed by multiplex genetic system analysis. The effect was reflected on the expressed proteins in the differentiated cells, where GMG-ITC caused increased in expression level of *Nrf2, SOD-1, NQO1, p52* and *c-Rel* of nuclear factor erythroid factor 2 (Nrf2) and nuclear factor kappa-B (NF-kB) pathways respectively. The findings revealed the potential of GMG-ITC to abrogate oxidative stress-induced neurodegeneration through Nrf2 and NF-kB signalling pathways.

Abbreviations: AD, Alzheimer's disease; ALS, Amyotrophic lateral sclerosis; Apaf-1, Apoptotic protease activating factor 1; ARE, Antioxidant response element; ATRA, All trans retinoic acid; BCA, Bicinchoninic acid; BSA, Bovine serum albumin; DMEM-F12, Dulbecco's Minimum essential Eagle Media; DMSO, Dimethyl sulfoxide; EDTA, Ethylenediaminetetraacetic acid; EMC7, Endoplasmic reticulum membrane protein complex subunit 7; FBS, Fetal bovine serum; GMG-ITC, Glucomoringin-isothiocyanate; GPI, Glucose-6-phosphate isomerase; HD, Huntington's disease; HPO or H2O2, Hydrogen peroxide; KanR, Kanamycin resistance gene; Mcl-1, Myeloid cell leukemia sequence 1 protein; MFI, Median fluorescence intensity; MYR, Myrosinase; MTT, 3-(4,5-Dimethylthiazol-2-yl)-2,5-diphenyltetrazolium bromide; NDD, Neurodegenerative diseases/ disorders; Nrf2, Nuclear factor erythroid 2-related factor 2; OligoCalc, Oligonucleotide properties calculator; p53, Cellular tumour antigen protein; PCR, Polymerase chain reaction; PD, Parkinson's disease; PSMB4, Proteasome subunit beta type 4; RIN, RNA integrity number; RIPA, Radioimmunoprecipitation assay; RNA, Messenger ribonucleic acid; ROS, Reactive oxygen species; RT, Reverse transcription; SAPE, Streptavidin phycoerythrin; SCI, Spinal cord injury; SH-SY5Y, Human neuroblastoma cell line; SNRPD3, Small nuclear ribonucleoprotein D3; Taq, Thermus aquaticus; XP, Extreme programming

* Corresponding author at: Laboratory of Molecular Biomedicine, Institute of Bioscience, Universiti Putra Malaysia, 43400, UPM Serdang, Selangor, Malaysia.
E-mail addresses: biojafar@kasu.edu.ng (M.S. Jaafaru), shariza@upm.edu.my (N. Nordin), rozita@upm.edu.my (R. Rosli), khozirah@upm.edu.my (K. Shaari), lady_h83@yahoo.com (H.Y. Bako), norazalina@upm.edu.my (N. Saad), noramaliza@upm.edu.my (N.M. Noor), madfaizal@upm.edu.my (A.F. Abdull Razis).

https://doi.org/10.1016/j.neuro.2019.09.008
Received 6 May 2019; Received in revised form 7 September 2019; Accepted 9 September 2019
Available online 12 September 2019
0161-813X/

1. Introduction

Neurodegeneration is a term used to describe disease conditions associated with nerve cells' deterioration (Solanki et al., 2016). The condition is characterised by progressive damage of neuronal cells with eventual loss of structure and function that leads to death (Kovacs, 2016; Toffa et al., 2019). This deteriorative condition result in gradual loss of cognitive functions including but not limited to memory and decision making (Solanki et al., 2016; Sharma et al., 2018). Neuronal degeneration is the driving force for a hundred of non-communicable disease conditions classified as neurodegenerative diseases (NDDs), many of which are neglected due to lower occurrence factor (Chen et al., 2017). The disease conditions express clinical and pathological feature heterogeneously distinctive to neurons, slowing down their functions and distorting anatomical systems of nerve cells (Kumar and Singh, 2015). NDDs conditions emerged for unclear reasons and progress in a persistent manner through a phenomenon that are poorly understood (Brettschneider et al. 2015). As a multi-systemic condition influenced by numerous biomarkers, NDD comprised of number of pathways that modulate various cellular and molecular processes including energy regulation, stress and inflammatory responses, protection of molecular/genetic damages, regulation of iron homeostasis, adaptation and metabolic regulations (Kovacs, 2016). As such, defect in any key metabolite in the pathway(s) result in severe pathological condition with consequent cell death (Kovacs, 2016).

Multiple number of studies described the involvement of oxidative stress and reactive oxygen species (ROS) in cellular damage with eventual death as explained earlier (Xu et al., 2015; Raina and Sen, 2018; Richards et al., 2018). Rising of ROS production in neuronal cells increase the blood-brain barrier permeability, synaptic transmission perturbation and tubulin changes, thereby reducing the chances of cells survival (Baxter et al., 2006; Sahin et al., 2017). Likewise, oxidation of fundamental macromolecules such as lipid, proteins and nucleic acids in the cells due to oxidative condition, alters their structure and functions. Such alterations result in the activation of several pathological signalling pathways, leading to neuronal cell death via apoptosis (Liu et al., 2015).

However, plant source natural and synthetic bioactive compounds with wide therapeutic potentials continue to fascinate the interest of life science researchers (Razis et al., 2011; Jaafaru et al., 2017, 2018a, 2018b; Waziri et al., 2018; Santana-Gómez et al., 2018) especially those focusing on neuronal regeneration and protection (Abdull et al., 2014; Jaafaru et al., 2018b; Singh et al., 2019). Glucomoringin-isothiocyanate (GMG-ITC) is a derivative of glucomoringin (GMG), a rare glucosinolate found mainly in *Moringa oleifera* Lam tree (Karim et al., 2016). The compound was reported to demonstrate wide spectrum biological activities such as anti-oxidant (Rajan et al., 2016), anti-inflammatory (Galuppo et al., 2014; Jaja-Chimedza et al., 2017), antimicrobial (Galuppo et al., 2013), anticancer (Michl et al., 2016) and anti-ulcerative (Karim et al., 2016) conditions. Studies on various neurodegenerative diseases involving suitable disease model of interest have shown that GMG-ITC attenuated damages in spinal cord injury (SCI) (Giacoppo et al., 2015), ameliorated certain abnormalities in focal ischemia (Galuppo et al., 2015a) and slowed down disease phenotype in amyotrophic lateral sclerosis (Galuppo et al., 2015b). The compound had gained tremendous attention in recent years as a promising candidate for neuronal protection. To unveil its potentials the more, we therefore investigated the influential effect of the GMG-ITC on the expression level of key genes and proteins involved NF-kB, Nrf2 and MAPK signalling pathways in an in vitro model of NDD, generated from terminally differentiated neuronal cells and hydrogen peroxide.

2. Materials and methods

2.1. Isolation and bio-activation of glucomoringin

Glucomoringin (GMG) was obtained from *Moringa oleifera* Lam seeds and bioactivated in accordance with the protocol reported in our previous studies (Jaafaru et al., 2018c). Briefly, GMG was isolated from methanol extract of *M. oleifera* Lam seeds using ion exchange chromatographic system and purified by gel filtration. The isolated GMG was characterised by means of proton (^{1}H), carbon (^{13}C) and two-dimensional (2D) Nuclear Magnetic Resonance (NMR) spectrometry. The purity of the compound was ascertained through High Performance Liquid Chromatographic (HPLC) analysis of desulfo-derivatives in line with ISO (International Standard Organisation) 91671 method approved by European Union commission regulation, EEC No 1864/90. Molecular weight of GMG was identified using electrospray ionization (ESI) in positive mode. However, purely isolated GMG was bioactivated by dissolving 1 mg of the compound in 1 mL PBS at pH 7.2 and incubated with 20 µL of myrosinase enzymes (Sigma Aldrich) at 37 °C. The complete hydrolysis of GMG to GMG-ITC was confirmed by HPLC and LC-MS (Liquid Chromatographic Mass Spectroscopic) analysis employing sinigrin as internal standard as described by Galuppo et al. (2013).

2.2. Cell culture

The cell lines used in the presence study was neuroblastoma SH-SY5Y (ATCC® CRL-2266™) cell obtained from UKM Medical Molecular Biology Institute (UMBI), Kuala Lumpur, Malaysia. The cells were maintained in a mixture of Dulbecco's Modified Eagle and Hams' 12 Media (DMEM/Hams' F12) in ratio 1:1, containing 10% fetal bovine serum (FBS), 1% (10,000 unit/mL of penicillin and 10,000 µg/mL of streptomycin), 1% 2 mM nonessential amino acid (L-Glutamine) and incubated in 5% CO_2 and 95% humidified atmospheric air at 37 °C. All the media components were procured from Nacalai, Kyoto, Japan.

2.3. Differentiation of SH-SY5Y cells

Differentiation of SH-SY5Y cells was achieved in accordance to the stipulated protocol outlined in our previous publication (Jaafaru et al., 2018c). To be precise, the cells were seeded in 6-wells plates at a density of 1×10^3 cells/mL for 24 h. 2 mL of differentiating media (DMEM/Hams' F12, 3% heat inactivated FBS and 10 µM all trans retinoic acid (RA)) was added to each well in the dark after 24 h of incubation. The plates were covered with sterile aluminum foil and incubated in 5% carbon dioxide (CO_2) incubator at 37 °C. Differentiating media was changed consecutively for a period of 10 days. After completion, RA-induced differentiation was evaluated under phase contrast in an inverted light fluorescence microscope (Zeiss Axio Vert A1, Germany) equipped with image acquisition system (AxioCam MRm, Germany). Multiple images were captured independently at different magnification. The differentiation was further confirmed by immunocytochemistry technique and flow cytometric assay where expression of neuron and synapse specific marker tuj-1 and synaptotagmin-1 were detected by means of Alexa fluor 488 and FITC-conjugated anti rabbit secondary antibodies.

2.4. Cytotoxicity and cell viability assays of GMG-ITC

Cytotoxicity of GMG-ITC and H_2O_2 were assessed using MTT reduction assay in accordance with modified protocol reported by Ismail et al. (2014). SH-SY5Y cells were seeded at a density of 1.0×10^3 cells/mL in 96-wells plate and differentiated as described in section 2.3. The cells were incubated with serially diluted concentration of GMG-ITC (0.156–10) µg/mL for 24, 48 and 72 h leaving the last two rows for enzyme control (myrosinase treatment) and normal control group

respectively. A 20 µL MTT (5 mg/mL) solution was added and incubated in the dark for 4 h after which the reagent was replaced with 200 µL DMSO to solubilize the formazan formed in the wells. Absorbance was recorded on microplate reader (Synergy, BioTek, USA) at 540 nm. Similar analysis was carried out for hydrogen peroxide (H_2O_2), where 1 mM H_2O_2 was considered the starting concentration for serial dilution. However, cell viability effect of GMG-ITC was ascertained when the differentiated cells were pre-treated with serially diluted GMG-ITC (µg/mL) in time dependant manner. The pre-treated cells were challenged with 300 µM (IC_{50}) H_2O_2 thereafter followed by the addition of MTT solution and DMSO accordingly as described above. Absorbance reading was measured at 540 nm on microplate reader. All the MTT experiments were conducted in triplicates under aseptic condition.

2.5. GMG-ITC pre-treatment and H_2O_2 exposure

The differentiated neuronal cells were seeded at a density of 1×10^3 cell/mL in T25 flask and differentiated as described above. The cells were pre-treated separately with 1.25 µg/mL GMG-ITC, 2.2 µg/mL of curcumin as positive control and 20 µL myrosinase as enzyme control for 72 h. The pre-treated cells were then challenged with 300 µM hydrogen peroxide (H_2O_2) for four hours prior to bioassay analyses.

2.6. Gene expression study of GMG-ITC treated neuron cells

This section comprised of various techniques employed to monitor the effect of GMG-ITC pre-treatment on genes' expression levels in differentiated neuronal cells with respected nuclear factor erythroid 2-related factor 2/antioxidant response element (Nrf2/ARE), nuclear factor kappa B-cell (NF-kB/IkB) and mitogen activated protein kinase (MAPK) signaling pathways.

2.6.1. Extraction of total ribonucleic acid (RNA)

Following differentiation and treatment, genomic RNA was isolated using total RNA extraction kit (Geneaid Biotech Ltd, Taipei, Taiwan) according to the manufacturer's protocol enclosed in the kit. The purity and amount of the isolated RNA were determined using Nano drop spectrophotometer (Thermo Scientific, USA). Meanwhile, the quality was determined by means of RNA integrity number using Agilent 2100 Bioanalyzer (Agilent Technologies, Waldbronn, Germany).

2.6.2. Primer design for gene expression

Genome Lab eXpress Profiler Software (Beckman Coulter, USA) was utilized for designing of primers as presented in Table 1, considering human sequence on the National Centre for Biotechnology Information Gene Bank Database (NCBI). The application was used to design all the genes of interest which include *NF-kB, BACE1, IkB, APP, Erk ½, JNK, P38, MKP1, PP2A, PP5, p53, Nrf2, GST, NQO1, GCL, Keap1, SOD1, SOD2, HO-1 and catalase.* The house keeping genes used in the experiment were *GPI, EMC7, PSMB4, SNRPD3, VCP*, while KanR was served as an internal control. Quality of the designed primers was ascertained on OligoCalc, an online software for complementarity checking. The primers were synthesized by Apical Scientific (Selangor, Malaysia) and diluted with 1 × Tris-EDTA buffer to the working concentration (100 nM) for both forward and reverse primers. The diluted primers were stored at 30 °C until required.

KanR was used as internal control. *NF-Kb*, Nuclear factor kappa B; *BACE1*, β-site amyloid precursor protein cleaving enzyme; *IkB*, inhibitory kappa B protein; *APP*, amyloid precursor protein; *MAPT*, Total-Tau protein; *Erk ½*, extracellular signal regulating protein kinase ½; *JNK*, C-Jun N-terminal kinase; *P38*, 38 subunit protein; *MKP1*, MAPK phosphatase; *PP2A*, serine/threonine protein phosphatase 2A; *PP5*, protein Phosphatase 5; *Bax*; Bcl_2 associated x protein; *Bcl_2*, β-cell lymphoma 2; *Apaf-1,* apoptotic protease activating factor 1; c*yt-C*, Cytochrome complex; *CASP3*, cysteine aspartic acid protease 3; *CASP8*, cysteine aspartic acid protease 8; *CASP9*, cysteine aspartic acid protease 9; *p53*, tumour suppressor gene; *Nrf2*, nuclear factor erythroid 2-related factor 2; *GST*, glutathione S transferase; *NQO1*, NADP Quinone oxidoreductase 1; *GCL*, glutamate cysteine ligase; *γGCS*, gamma glutamylcysteine synthetase; *SOD1*, superoxide dismutase 1; *SOD2*, Mn-dependant superoxide dismutase; *Catalase*, *UGT*, *UDP-glucuronosyltransferase*; *HO-1*, hem oxygenase-1; *EMC7*, ER membrane protein complex subunit 7; *GPI*, glucose-6-phosphate isomerase; *PSMB4*, proteasome subunit beta type 4; *SNRPD3*, small nuclear ribonucleoprotein D3; *VCP*, valosin containing protein.

2.6.3. Reverse transcription reaction and polymerase chain reaction

The reverse transcription reactions (RT) and polymerase chain reactions (PCR) were conducted in an XP Thermal Cycler (BIOER Technology, Hangzhou, China) in accordance with GenomeLab™ GeXP start kit (Beckman Coulter, US). Briefly, the reaction mixture for RT was prepared by adding 1 µL of isolated genomic RNA sample (50 ng/µL) to the master mix comprising 11 µL DNAse/RNase free water, 4 µL RT buffer (5 ×), 2.5 µL RT reverse primers, 1 µL reverse transcriptase and 1 µL KanR. The mixture was introduced to the thermal cycler and cDNA was synthesized according to the following reaction conditions: 48 °C for 1 min, 42 °C for 60 min, 95 °C for 5 min and the product was hold at 4 °C after completion. On the other hand, 9.3 µL of RT product was introduced to PCR master mix which constitute of 4 µL PCR buffer (5 ×), 4 µL MgCl, 2 µL PCR forward primer and 0.7 µL thermostat DNA polymerase. The combined volume of the mixture was subjected to PCR, considering 95 °C and 10 min as amplification condition. The reaction was completed after 1 h 56 min following 34 cycles of 94 °C for 30 s, 55 °C for 30 s, 70 °C for 1 min and was finally hold at 4 °C.

2.6.4. Gene expression and data analysis

The reaction mixture for GeXP was prepared by introducing 1 µL of PCR product to the master mix solution containing 38.5 µL sample loading solution and 0.5 µL DNA standard size in 96 well sample loading plates and covered with a drop of mineral oil to prevent evaporation of the contents. After analyzing the mixture on GeXP machine using fragment analysis module of the GeXP system software, the outcome was exported to analysis module of eXpress profiler software and processed further, where KanR was used for accomplishing the normalization.

2.7. Protein quantification assay

The cells were seeded in 6-well plates at a density of 1×10^3 cell/mL, differentiated and treated as described in section 2.3 and 2.5.3 and 2.5 respectively. The neuron cells were washed with 1 × cold PBS twice followed by addition of 500 µL protease inhibitor containing RIPA buffer (Nacalai Tesque, Japan), and stirred slowly. After 5 min, the cells were scrapped out with plastic cell scrapper and transferred to a fresh centrifuge tube. The protein lysates were vortexed briefly on EVT 3000 vortexing device (Bio Tek, Winooski, VT, USA) and incubated on ice for 20 to 30 min according to the manufacturer's protocol. The suspensions were then centrifuged at 10,000 × *g* for 10 min at 4 °C, and the supernatants were transferred to a new tube and kept on ice. BCA protein quantification assay kit (Nacalai Tesque, Japan) was used to quantify the protein contents in the extract by mixing 25 µL of the extracts and 200 µL of combined volume of solution A and B in ratio 50:1. Serially diluted 2 mg/mL bovine serum albumin (BSA) was used to plot standard curve for quantification of the isolated proteins. The 96 well plate was incubated at 37 °C for 30 min. and absorbance reading was taken at 562 nm thereafter. The unknown protein concentrations were calculated from the plotted standard curve of BSA.

2.7.1. Sodium dodecyl sulphate-polyacrylamide gel electrophoresis

The extracted protein samples were separated by electrophoresis on GoPAGE 5–11 % precast sodium dodecyl sulphate-polyacrylamide gel

Table 1
Accession numbers, genes' names and universal nucleotides for the primers used in the present study.

	Sequence of primers with universal tags	
Gene and [accession no]	Forward primers (5'→3')	Reverse primers (3'→5')
AKT3 [NM_005465.4]	AGGTGACACTATAGAATAAGACATTAAATTTCCTCGAA	GTACGACTCACTATAGGGAATCCTCATCATATTTTTCAGGT
APP [NM_000484.3]	AGGTGACACTATAGAATACTGTGGCAGACTGAACATGC	GTACGACTCACTATAGGGATCACCAACTAAGCAGCGGTA
BACE1 [NM_012104.4]	AGGTGACACTATAGAATACGAGCTGGATTATGGT	GTACGACTCACTATAGGGAGGAGAGGGAGCTTGG
Catalase [NM_001752.3]	AGGTGACACTATAGAATAAGAAATCCTCAGACACATCT	GTACGACTCACTATAGGGAATGTCATGACCTGGATGTAA
GCLC [NM_001498.3]	AGGTGACACTATAGAATAATGAAGCAATAAACAAGCAC	GTACGACTCACTATAGGGATGGAATGTCACCTGGAG
GST [NM_015917.2]	AGGTGACACTATAGAATAATACATGGCAAATGACTTAAA	GTACGACTCACTATAGGGATGATGTCTTCATTCCTTGAC
HO-1 [NM_002133.2]	AGGTGACACTATAGAATAACTGCGTTCCTGCTCAACAT	GTACGACTCACTATAGGGAGGGCAGAATCTTGCACTTTGT
IKBA [NM_020529.2]	AGGTGACACTATAGAATACTGCAGCAGACTCCAC	GTACGACTCACTATAGGGAGGGTATTTCCTCGAAAGT
JNK [NM_001323327.1]	AGGTGACACTATAGAATAAAGGAAAACGTGGATTTATG	GTACGACTCACTATAGGGACCAGCATATTTAGGTCTGTT
MAPT [NM_001123066.3]	AGGTGACACTATAGAATACCCAGATCTGAGAGAGGT	GTACGACTCACTATAGGGACTTATTAATTATCTGCACCTTCC
MKP1 [NM_004417.3]	AGGTGACACTATAGAATAAGAAGAACCAAATACCTCAA	GTACGACTCACTATAGGGACAGGTCATAAATAATCAGCA
NF-kB [NM_002908.3]	AGGTGACACTATAGAATACGTTTTAGATACAAATGTGAAG	GTACGACTCACTATAGGGACACTTTTCCTTTTCCATAAT
NQO1 [NM_000903.2]	AGGTGACACTATAGAATACTGCGAACTTTCAGTATCC	GTACGACTCACTATAGGGAGAAGGGTCCTTTGTCATAC
Nrf2 [NM_006164.4]	AGGTGACACTATAGAATATCGCAAACAACTCTTTATCT	GTACGACTCACTATAGGGAAGAGGAGGTCTCCGTTA
p38 [NM_001315.2]	AGGTGACACTATAGAATATGAGCTGAAGATTCTGGA	GTACGACTCACTATAGGGATGTCAGACGCATAATCTG
p53 (TP53) [NM_000546.5]	AGGTGACACTATAGAATAATGGAAACTACTTCCTGAAA	GTACGACTCACTATAGGGAATTCTGGGAGCTTCATCT
PP5 [NM_006247.3]	AGGTGACACTATAGAATACAAGGACTACGAGAACGCCA	GTACGACTCACTATAGGGAGCTTCACCTTGACCACCGTC
PP2A [NM_002715.3]	AGGTGACACTATAGAATACCGCCATTACAGAGAG	GTACGACTCACTATAGGGAAGGATTTCTTTAGCCTTCT
SOD1 [NM_000454.4]	AGGTGACACTATAGAATAAAGTACAAAGACAGGAAACG	GTACGACTCACTATAGGGATGACAAGTTTAATACCCATCT
SOD2 [NM_000636.3]	AGGTGACACTATAGAATAACAACAGGCCTTATTCC	GTACGACTCACTATAGGGAAGAGCTTAACATACTCAGCA
UGT [NM_000463.2]	AGGTGACACTATAGAATACCCATTCTCCTACGTG	GTACGACTCACTATAGGGACTTCAAATTCCTGGGATA
Housekeeping genes		
EMC7 [NM_020154.2]	AGGTGACACTATAGAATATCCTTAAGACAGATGGGAGT	GTACGACTCACTATAGGGAATTCACATATCTTGCTCTCA
GPI [NM_001184722.1]	AGGTGACACTATAGAATATCTGCAGCCTCCAAC	GTACGACTCACTATAGGGAAGTAATCCACCAGGATATG
KanR	ATCATCAGCATTGCATTCGATTCCTGTTTG	ATTCCGACTCGTCCAACATC
PSMB4 [NM_002796.2]	AGGTGACACTATAGAATATTCTGCTACCGTGACTAAG	GTACGACTCACTATAGGGATGATTGGACCTCTGTAAAGT
SNRPD3 [NM_004175.4]	AGGTGACACTATAGAATACGAAGAGAAGAAAAGTAGGC	GTACGACTCACTATAGGGATGACAAGTTTAATACCCATCT
VCP [NM_007126.4]	AGGTGACACTATAGAATACCCTTCCGATGATTC	GTACGACTCACTATAGGGAGGGTAACGGCTACGA

(SDS-PAGE) (SMOBIO Technology, Japan), at 200 V for 60 min. The samples were diluted with sample loading buffer in 1 to 1 dilution prior to loading and run in Tris running buffer medium containing 192 mM glycine, 5 mM Tris base, 0.1% SDS at pH 8.3.

2.7.2. Western blot and gel viewing

The resolved protein molecules from previously described SDS-PAGE analysis were transferred to polyvinylidene difluoride (PVDF) membrane (Bio-Rad, USA), employing semi dried transfer system. Briefly, the transfer was performed by sandwiching transfer buffer (192 mM glycine, 25 mM Tris and 20% methanol) pre-soaked filter papers, methanol activated PVDF membrane and trimmed proteins containing gel on Trans-Blot Turbo Transfer System (Bio-Rad, Singapore). The system was run for 5, 7, or 10 min at 1.3A and 25 V for low, mix or high molecular weight proteins respectively. The membrane was blocked in BlockingOne (Nacalai Tesque, Japan) at room temperature for 1 h on an orbital shaker (Heldolph, Germany) with low speed. It was washed 3 times for 5 min. each, with washing buffer (TBS-Tween 20) on an orbital shaker at moderate speed thereafter. Primary and secondary antibodies (Cell Signalling Technology, USA) were prepared in BlockingOne (Nacalai Tesque, Japan), both in ratio 1:1000 and kept at 4 °C. The membrane was incubated in primary antibody overnight at 4 °C and secondary antibody at 25 °C for 1 h on an orbital shaker with slow speed, followed by 3 times washing (5 min. each) with TBS-Tween 20 in between and after the incubations.

The membranes were further developed with chemiluminescence substrate (Nacalai Tesque, Japan) by adding 2 mL of a combined volume of solution A and B in ratio 1:1, according to the manufacturer's instruction. After 5 min. incubation, the membrane was drained carefully, covered in plastic and viewed using ChemiDoc™ Imaging System (Bio-Rad, USA), and protein expression was normalized with bands of beta actin (a housekeeping protein). The bands were analysed, and relative intensities were extracted on ImageJ (a free online image analysis software).

2.8. Statistical analysis

Data were presented as means ± standard deviation, differences between the means of test and control groups were determined by one-way analysis of variance (ANOVA) with Turkey's multiple compassion, on Statistical Package for Social Scientist software version 23.0 (SPSS Inc., Chicago, Illinois, USA). All the experiments were conducted three times (n = 3) independently and 95% confidence interval was considered, thus $p < 0.05$ referred to statistical significance.

3. Results

3.1. Characterization of isolated glucomoringin (GMG)

Following the extraction and isolation of the compound under study, H^1 & ^{13}C NMR based analysis revealed the molecular structure of sugar moieties in the isolated compound as seen in Table 2.

Analysis using two-dimensional NMR (2D NMR) spectroscopy techniques namely COSYad, HSQCad and HMBCad after isolation unveiled the components of the isolated compound as glucosyl, benzyl and rhamnosyl moieties. The outcome further described the semi-spatial molecular arrangement in the isolated compound (proton-carbon and proton-proton coupling), direct and indirect correlations among the protons on the anomeric and non-anomeric carbon atoms within the molecule. ^{13}C-NMR spectrum also showed the connection between benzyl molecules, sulphate group and sugar moiety through quaternary carbon atom. Likewise, the information from HMBC spectrum revealed the correlation between carbon 1 of rhamnosyl and that of benzyl ring that connect the two moieties together in the compound, as seen in Fig. 1.

Similarly, HPLC analysis showed a single compound eluted at around 9 min with an intensity of about 700,000 μγ (Fig. 2). Identification of the isolated compound was further confirmed by liquid chromatography mass spectrometry (LC-MS) using electron spray ionization (ESI) in positive mode, which yield *m/z* 588.4111 $[M+H]^+$

Table 2
^{1}H NMR and ^{13}C NMR data spectra for isolated glucomoringin.

Moieties	Isolated compound		de Graaf et al. (2015)	
	δC	δH (J in Hz)	δC	δH (J in Hz)
Glucose moiety				
1'	80.4	4.57, d, (8.9)	80.9	4.57, d, (9.0)
2'	71.9	3.17–3.36, m	71.9	3.17–3.30, m
3'	76.9	3.17–3.36, m	70.0	3.17–3.30, m
4'	68.9	3.17–3.36, m	68.8	3.17–3.30, m
5'	79.7	3.09, m	79.7	3.09, m
6'	60.2	3.49, m	60.2	3.50, m
Benzyl moiety				
1	154.5	———	154.4	———
2	117.5	7.00, d, (8.7)	117.4	7.00, d, (8.7)
3	129.4	7.19, d, (8.8)	129.3	7.18, d, (8.7)
4	130.6	———	130.4	———
5	129.4	7.21, d, (8.8)	129.3	7.18, d, (8.7)
6	117.5	7.00, d, (8.7)	117.4	7.00, d, (8.7)
7	37.4	3.86, d, (17.0)	37.2	3.86, d, (17.0)
Others				
0	154.5	———	154.6	———
Rhamnose moiety				
1''	98.0	5.41, d, (1.7)	98.1	5.41, d, (1.7)
2''	69.6	4.02, d, (1.7–3.6)	69.9	4.03, d, (1.7–3.5)
3''	69.9	3.86, d, (3.5–7.0)	70.0	3.86, d, (3.5–7.0)
4''	70.7	3.37, t, (9.6)	70.2	3.38, t, (9.7)
5''	69.3	3.66, m	69.3	3.67, m
6''	16.6	1.08, d, (6.2)	16.6	1.09, d, (6.3)

Where **d:** double peaks; **m:** multiple peaks; **t:** triplet peaks.

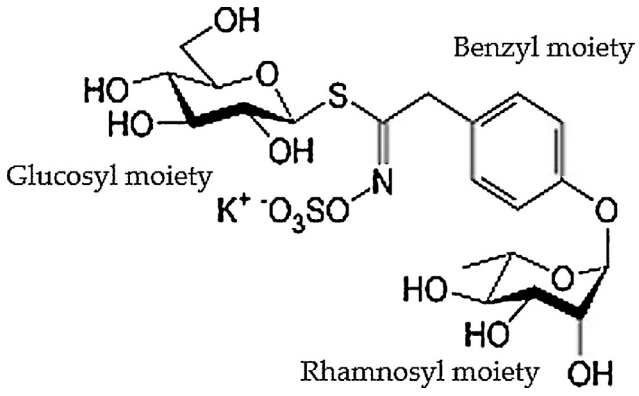

Fig. 1. Intact structure of glucomoringin (GMG) also known as 4-(α-L-rhamnosyloxy) benzyl, comprising of glucosyl, benzyl and rhamnosyl moieties.

(Fig. 3). The digits correspond to the mass of protonated glucomoringin reported by de Graaf et al. (2015). Thus, the collective outcomes of the above analysis and supporting data from literature (Table 2), enabled the unequivocal identification of the isolated compound as 4-(α-L-rhamnosyloxy) benzyl glucosinolate or glucomoringin (GMG). The isolated GMG was further activated to GMG-ITC (Fig. 4) by 20 µL myrosinase (a hydrolytic enzyme) at pH 7.2 to enable the subsequent bioassay experiments and the reaction was confirmed using HPLC as suggested by Galuppo et al. (2013).

3.2. Confirmation of RA-mediated differentiation of SH-SY5Y cells

Expression level of synaptotagmin-1 and NeuN was observed after 7 days of retinoic acid (RA)-mediated differentiation of human neuroblastoma (SH-SY5Y) cells, by means of immunoblotting as seen in Fig. 5. The result demonstrated the magnitude of differention of SH-SY5Y cells due to daily treatment of the cells with RA for 7 days in the dark, indicating significant ($p < 0.05$) expression of synaptotagmin-1, a synapse associated protein and NeuN which is a marker found specifically in matured neurons (Fig. 6). This confirmed that the cells used in the present study were terminally differentiated neuron cells.

3.3. Cytotoxicity of GMG-ITC and H_2O_2

GMG-ITC treatment was performed to evaluate its effect on cell viability. Although the GMG-ITC treated differentiated cells at various concentrations (0.313–10) µg/mL for 24 h (Fig. 7a), 48 h (Fig. 7b) and 72 h (Fig. 7c) were significantly ($p < 0.05$) viable in all respect, the viability of those treated with 10 µg/mL for 24 and 48 h as well as 5 and 10 µg/mL for 72 h were significantly ($p < 0.05$) lower compared to other concentrations. Cytotoxicity of H_2O_2 was also determined, where differentiated cells were exposed to H_2O_2 at different concentrations in time dependant manner. The result obtained showed that 300 µM H_2O_2 triggered the death of about 50% of the cell population in 4 h (Fig. 8). Therefore, it was selected as concentration of H_2O_2 to induce oxidative stress condition. Thus, NDD model was developed for the subsequent experiments.

3.4. GMG-ITC modulated gene expression in NF-kB/IkB pathway

Expression of genes involved in NF-kB/IkB-mediated neuropathological pathway was affected remarkably in an oxidative stress condition with or without presence of GMG-ITC and curcumin. The genes influencing the pathway includes *NF-kB, IkB, BACE1 (β-secretase)*, *APP* and *MAPT tau*. The expression level of all the genes was significantly higher ($p < 0.05$) in H_2O_2 and myrosinase control groups compared to normal control. Pre-treatment of differentiated cells with GMG-ITC for 72 h prevented over expression of *NF-kB* gene significantly ($p < 0.05$) when the cells were exposed to H_2O_2-induced cytotoxic environment for 4 h compared to its expression in H_2O_2 control cells (Fig. 9A). GMG-ITC pre-treatment prior to H_2O_2 exposure caused a significant ($p < 0.05$) increased in the expression level of mRNA for *IkB* gene in the differentiated neuron cells compared to H_2O_2 control cells (Fig. 9B). Significant decreased ($p < 0.05$) in the expression level of *BACE1* gene in GMG-ITC pre-treated cells prior to 4 h H_2O_2 exposure was observed when compared the expression in H_2O_2 control cells (Fig. 9C). Also, presence of GMG-ITC abrogated the expression of *APP* gene significantly ($p < 0.05$) when the differentiated neurons were pre-treated with the compound before the introduction H_2O_2, compared to its expression in H_2O_2 control cells (Fig. 9D). Likewise, pre-treatment with GMG-ITC for 72 h increased the expression of *MAPT tau* gene significantly ($p < 0.05$) in an oxidative stress condition when compared to its expression in H_2O_2 control cells without the compound pre-treatment (Fig. 9E).

3.5. GMG-ITC modulated gene expression in Nrf2/ARE pathway

The expression level of mRNA for all the genes in Nrf2/ARE signalling pathway under study increased significantly ($p < 0.05$) in GMG-ITC pre-treated plus 4 h H_2O_2 challenged differentiated neuron cells in comparison to that of H_2O_2 control cells (Fig. 10A to 10I). The expression of *Nrf2* genes increased above normal level due to GMG-ITC pre-treatment of the differentiated neuron cells (Fig. 10A). Similarly, pre-treatment of the cells with GMG-ITC with or without H_2O_2 challenge rise the mRNA level of *GST* gene significantly ($p < 0.05$) compared to H_2O_2 and control (Fig. 10B). Level of *NQO1* gene expression in GMG-ITC pre-treated and H_2O_2 exposed differentiated cells increased significantly ($p < 0.05$) in comparison to H_2O_2 control cells (Fig. 10C). GMG-ITC pre-treatment prior to H_2O_2 exposure caused significant ($p < 0.05$) increased in the expression of *GCLC* gene in the differentiated neuron cells compared to H_2O_2 control cells (Fig. 10D). Expression of *SOD1* gene was also increased significantly ($p < 0.05$) in the differentiated cells due to GMG-ITC pre-treatment before H_2O_2 insult when compared to that of H_2O_2 control cells (Fig. 10E). Similar trend of expression ($p < 0.05$) was equally noticed with respect to *SOD2* gene (Fig. 10F). Presence of GMG-ITC elevated the expression

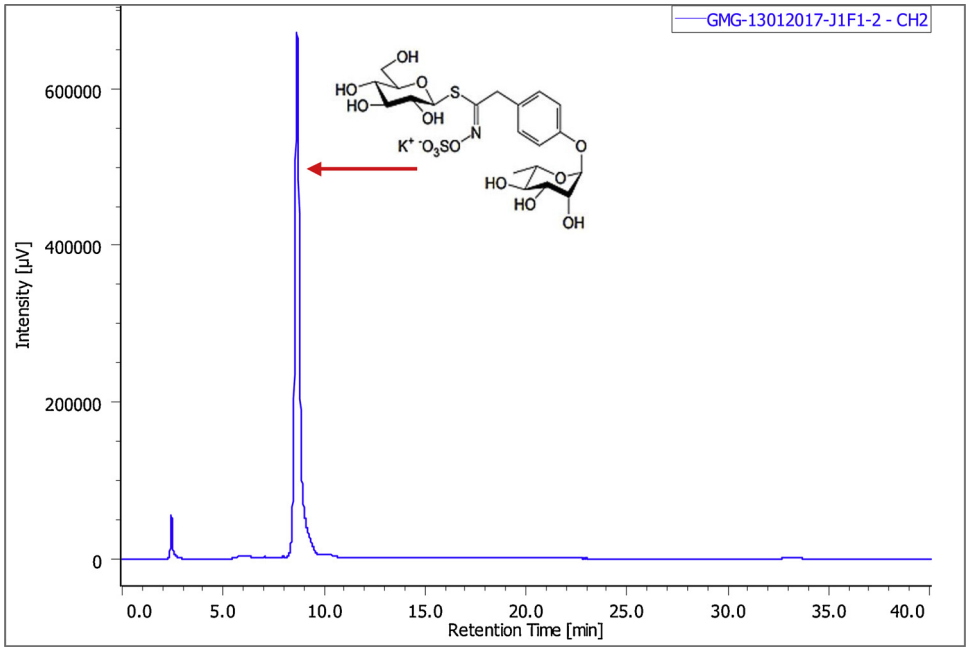

Fig. 2. HPLC chromatogram of isolated glucomoringin (GMG). This indicated that GMG was isolated in high purity from the 70% methanol extract of *M. oleifera* Lam seed's sample.

level of mRNA for *HO-1* and *Keap 1* gene expression significantly ($p < 0.05$) when the differentiated neuron cell was pre-treated with the compound before introducing H_2O_2 to the flask (Fig. 10G and H). Moreover, the level of mRNA for *catalase* gene expression increased significantly ($p < 0.05$) in similar pattern with other phase II antioxidant markers when the differentiated cells pre-treated with GMG-ITC for 72 h and subjected to 4 h H_2O_2 challenged, compared to its expression in H_2O_2 control cells (Fig. 10I).

3.6. GMG-ITC modulated gene expression in MAPK pathway

Although treatment of differentiated SH-SY5Y cells with 300 µM H_2O_2 significantly ($p < 0.05$) altered the expression level of mRNA for all the genes i.e. *JNK, p38, MKP-1, PP2A, PP5* and *Erk1/2* in MAPK signaling pathway, GMG-ITC pre-treatment seemed ineffective in antagonizing the genotoxic effect of the toxicant (Fig. 11). Pre-treatment of the differentiated cells with GMG-ITC for 72 h did not banish the overexpression of *JNK* in an oxidative stress condition and the different in expression was not significant ($p > 0.05$) when compared to that of H_2O_2 control cells (Fig. 11A). Meanwhile curcumin (positive control) on the other hand slow down the expression significantly ($p < 0.05$) when pre-treated the differentiated cells with it for 72 h before H_2O_2 challenged (the same figure). Unlike GMG-ITC, present of curcumin (positive control) in the cells prior to H_2O_2 exposure significantly ($p < 0.05$) reduced the expression level of *p38* gene compared to that of H_2O_2 control cells (Fig. 11B). Significant ($p < 0.05$) decreased in the

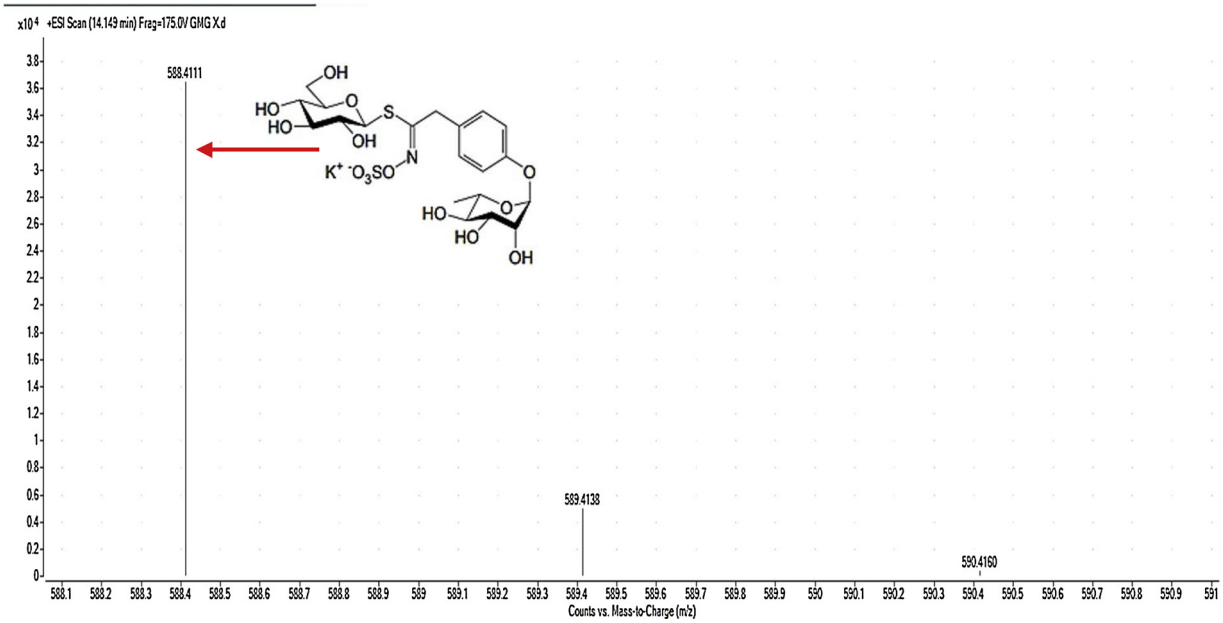

Fig. 3. LC-MS ESI (positive mode) spectrogram of isolated glucomoringin (GMG). The analysis confirmed the isolation of GMG in high purity by revealing its molecular weight (588.4111 *m/z*) in positive mode, together with few fragments of the compound.

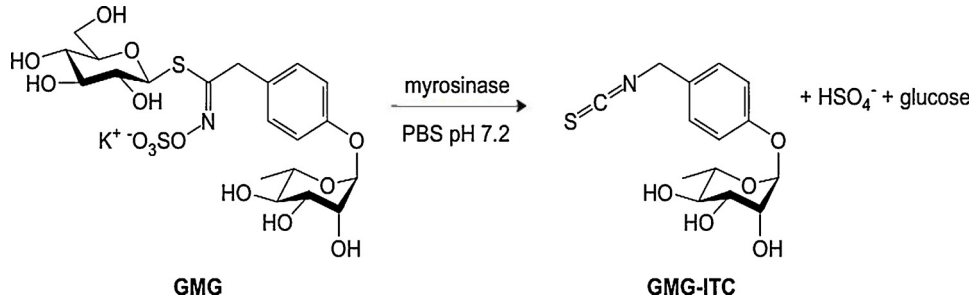

Fig. 4. Myrosinase catalysed hydrolysis of GMG to GMG-ITC. 4-(α-L-rhamnosyloxy) benzyl glucosinolate known as glucomoringin is hydrolysed to 4-(α-L-rhamnosyloxy) benzyl isothiocyanate or glucomoringin isothiocyanate by myrosinase in phosphate buffered solution (PBS) at pH 7.2.

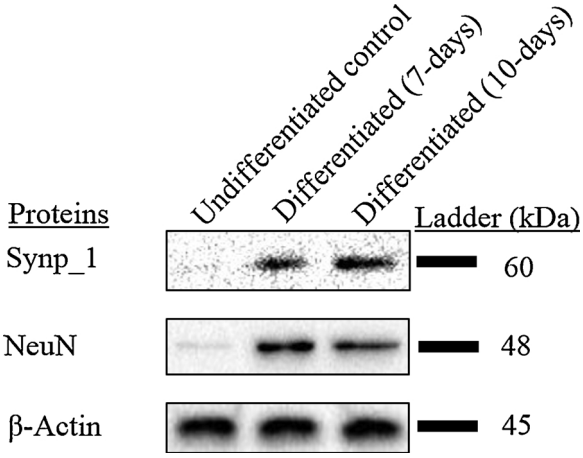

Fig. 5. Immunoblot based expression of terminal neuron-specific and synapse associated protein markers (NeuN and Synaptotagmin-1) in differentiated human neuroblastoma (SH-SY5Y) cell lines. Normalised against housekeeping protein (β-actin).

expression level of *MKP-1* gene was observed in the differentiated cells pre-treated with GMG-ITC for 72 h and subjected to 4 H_2O_2 treatment compared to the expression in H_2O_2 control cells (Fig. 11C). Presence of GMG-ITC in the differentiated cells did not affect the expression of *PP2A* and *PP5* genes significantly ($p > 0.05$) compared to normal control cells. Likewise, pre-treatment of the cells with GMG-ITC for 72 h prior to H_2O_2 insult failed to prevent the genotoxic effect of H_2O_2 on the expression level of the two genes (Fig. 11D and E). Although not significant ($p > 0.05$) the expression level of *Erk1/2* gene slightly decreased in the differentiated cells pre-treated with GMG-ITC for 72 h and H_2O_2 for 4 h compared to H_2O_2 control cells (Fig. 11F).

3.7. Expressions of selected proteins modulated by GMG-ITC

Immunoblotting was performed on the pre-treated differentiated neuronal cells to monitor the expression of important proteins responsible for neuroprotective and survival effect in the signalling pathways under study. The results showed that pre-treatment with GMG-ITC caused remarkable resistance to H_2O_2 cytotoxic effect on expression of the key proteins involved in phase II detoxification processes (Nrf2, NQO1 and SOD1), despite the induction of oxidative stress condition (Fig. 10). Similarly, the curcumin (positive control) affected the expression of all the proteins positively except the Nrf2. Following normalization with housekeeping protein (β-actin), the quantitative data were presented as relative intensity of proteins of interest to housekeeping protein, expressed in fold changes (Fig. 12), for quantitative evaluation of the protein expression. The results also confirmed the expression of c-Rel and p52 proteins, the two-constitutive transcription factor subunit in NF-kB pathway that enhance protection and survival of nerve cells. The expression level of the proteins was significantly high ($p < 0.05$) in GMG-ITC pre-treated compared to H_2O_2 control differentiated cells. Relative expression of c-Rel was measurably higher in GMG-ITC and curcumin control cells, and lower expression level of the protein in H_2O_2 control indicated the influence of GMG-ITC on the protein's expression (Fig. 13).

4. Discussion

The present study described novel mechanistic pathways for GMG-ITC neuroprotection activities against H_2O_2-induced

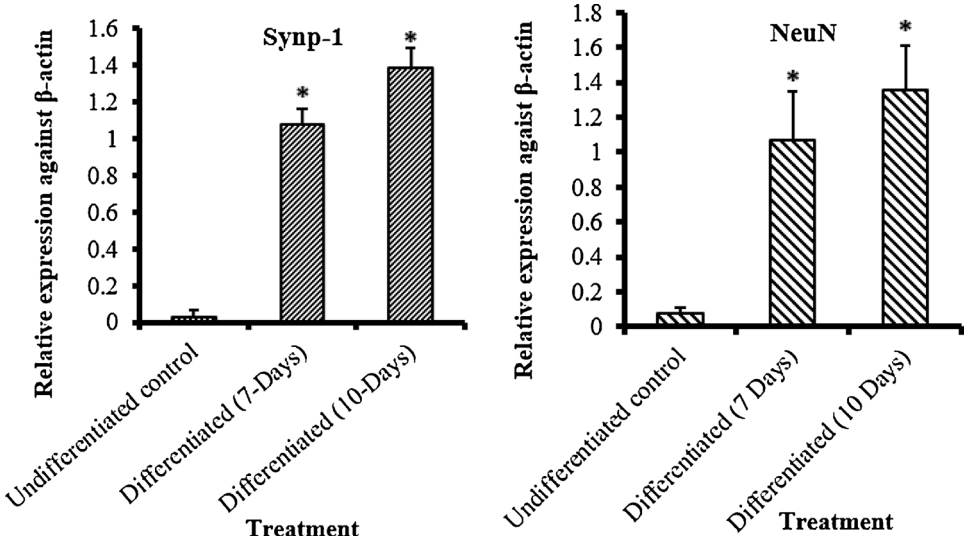

Fig. 6. Intensity based relative expression of terminal neuron-specific and synapse associated markers (NeuN and Synaptotagmin-1) after 7 and 10 days of retinoic acid-induced differentiation in human neuroblastoma (SH-SY5Y) cell lines. Normalised against β-actin housekeeping protein. Error bars represent standard deviation, means with asterisk differed significantly with control at 95% confidence level *(ANOVA, $p < 0.05$).

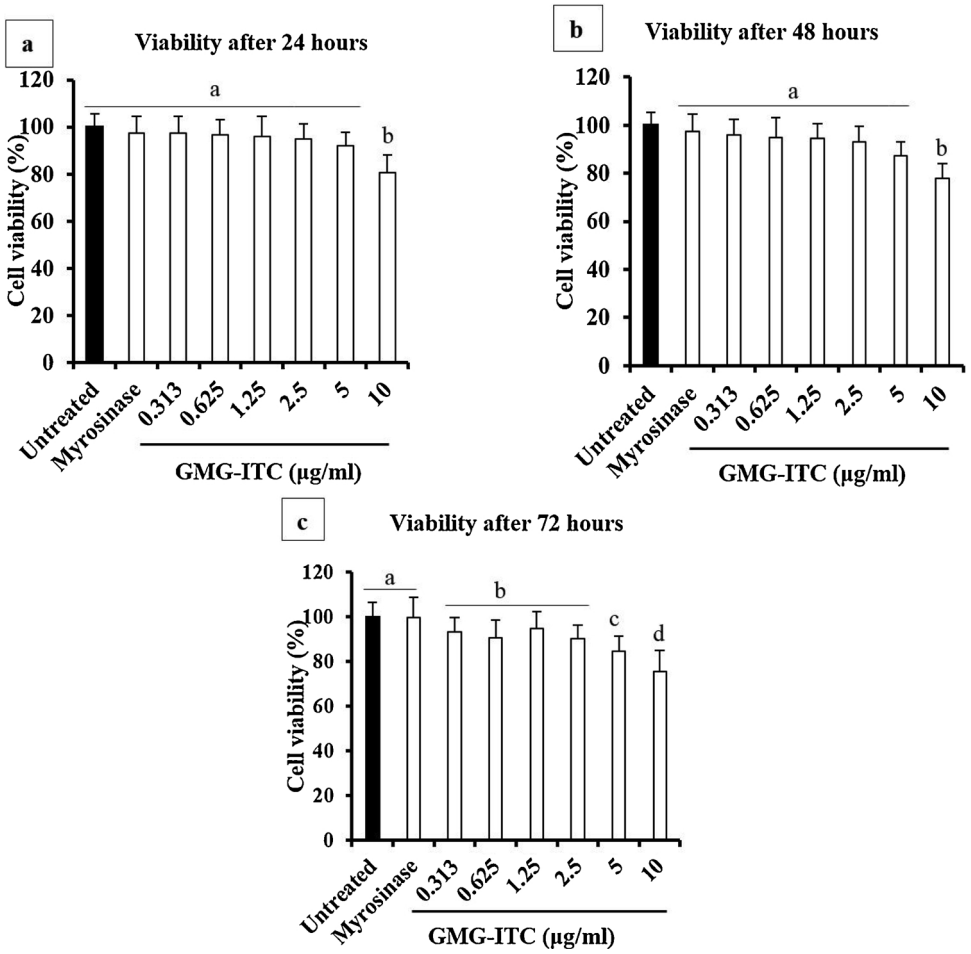

Fig. 7. Cytotoxicity of GMG-ITC on differentiated SH-SY5Y. (a) displayed 24, (b) 48 and (c) 72 h of treatment. Values are means of triplicate experiments and means with different letters varies significantly ($p < 0.05$, $n = 3$) with one another.

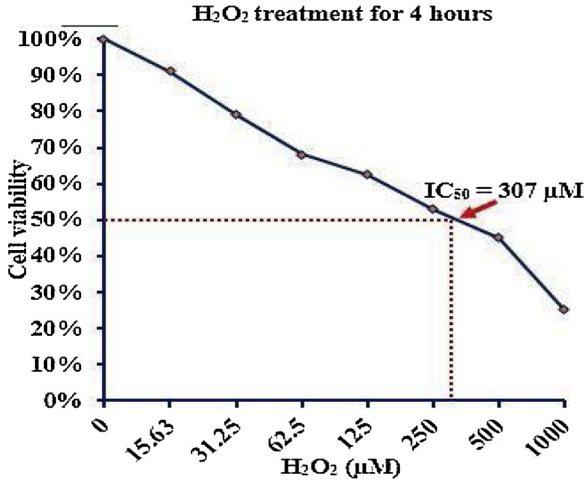

Fig. 8. Cytotoxicity of H_2O_2 on differentiated SH-SY5Y. The figure displayed the cytotoxic analysis result of H_2O_2, where 307 µM of the chemical appeared to kill 50% of the cells population with four (4) hours. The concentration was referred to as IC_{50} for generating oxidative stress model on differentiated SH-SY5Y cells. Experiments were conducted in triplicates (n = 3).

neurodegeneration. Due to its richness in bioactive compounds, *M. oleifera* plant exhibited wide range of biological activities and health benefits including but not limited to anti-inflammatory, antidiabetic, anticancer, antimicrobial and wound healing (Abdull et al., 2014; Al-Asmari et al., 2015; Kumssa et al., 2017). Human neuroblastoma cells (SH-SY5Y) are dopaminergic neuronal cells that gain popularity as a model for neurodegenerative diseases such as Alzheimer's disease (AD), Parkinson's disease (PD), multiple sclerosis (MS), amyotrophic lateral sclerosis (ALS) and Huntington's disease (HD) (Kim et al., 2013; Mangieri et al., 2014; Mastrantonio et al., 2016). Studies have shown that the cells differentiated into terminal neurons by showing not only neurites extension but expression of certain neuron specific markers such as synaptotagmin-1 and NeuN. This is achieved when the cells were incubated with 10 µM all-trans retinoic acid (RA) or other differentiating inducers at effective concentrations for appropriate number of days (Korecka et al., 2013; Ferguson and Subramanian, 2016). Although, increase predisposition of the cells to cytotoxicity during differentiation process was reported, SH-SY5Y cells were differentiated to neurons with features of fully matured neuronal cells by expressing neuron and synapse specific proteins which include class III β-tubulin (tuj-1), NeuN and synaptotagmin-1 (Cheung et al., 2009). The differentiation results confirmed that the cells used in the presence study were terminally differentiated neuronal cells.

Moreover, Studies have shown that subjecting differentiated SH-SY5Y cells to cytotoxicants such as hydrogen peroxide for certain period triggers cascade of reaction that lead to oxidative stress condition with eventual death of the cells (Chen et al., 2009). Ismail et al. (2016) and Park et al. (2015) reported the cytotoxic effect of H_2O_2 on differentiated SH-SY5Y cells when used as a model for neuroprotection research.

Following pre-treatment of differentiated neurons with GMG-ITC, expression of key genes in the studied pathways were affected remarkably as described in the result section. Studies have shown that

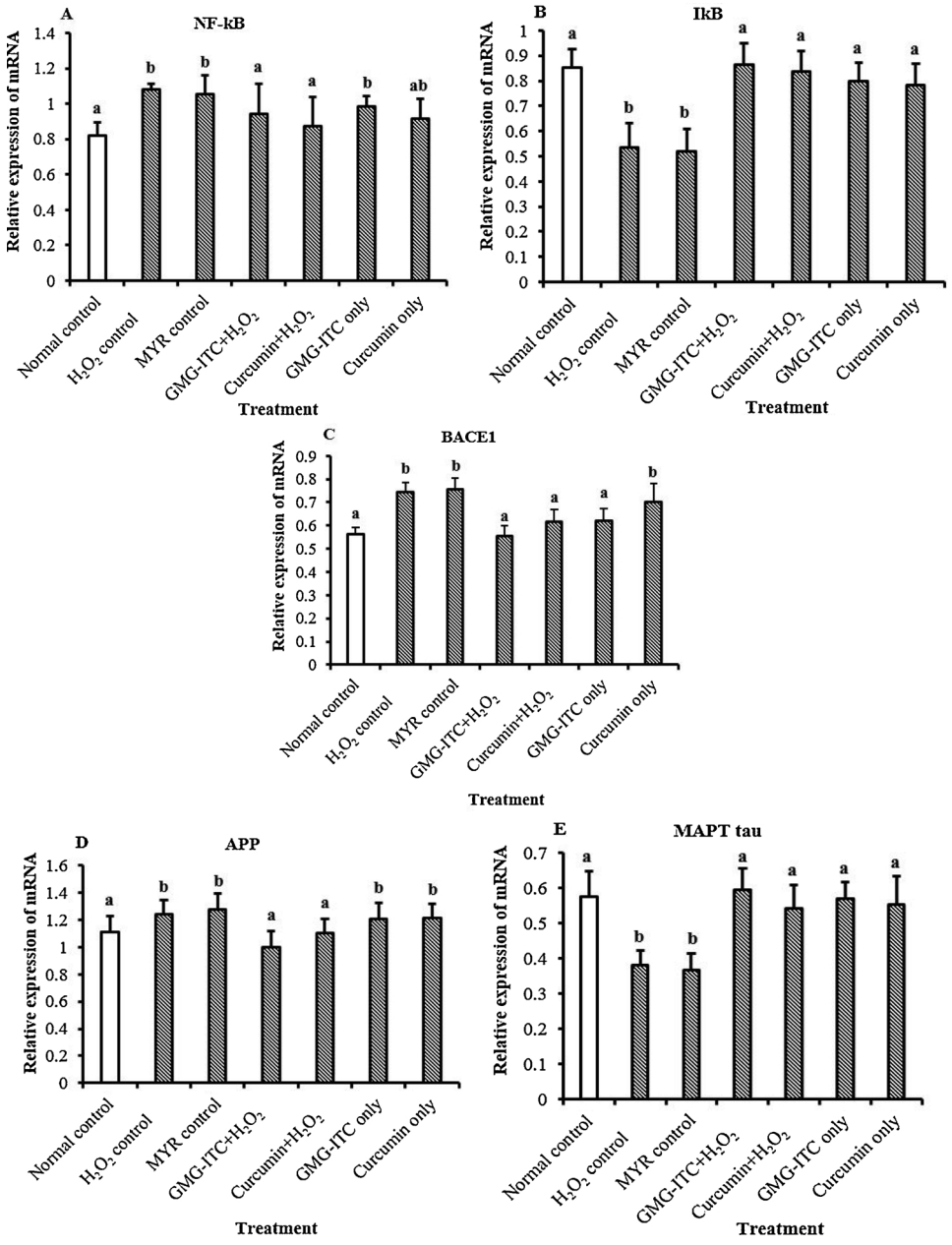

Fig. 9. Modulation of gene expression in NF-kB/IkB signalling pathway. Where normal control is a group of untreated cells; H_2O_2: cells treated with 300 μM hydrogen peroxide only for 4 h; MYR control: myrosinase (enzyme) pre-treated and hydrogen peroxide exposed group; GMG-ITC + H_2O_2: cells pre-treated with GMG-ITC for 72 h followed by 4 h exposure to hydrogen peroxide; curcumin + H_2O_2: cells pre-treated with curcumin followed by exposure to hydrogen peroxide for 4 h; GMG-ITC only: and curcumin only: cells treated with only GMG-ITC and curcumin for 72 h respectively. GMG-ITC: glucomoringin isothiocyanate; H_2O_2: hydrogen peroxide; MYR: myrosinase. The result was expressed as relative expression of mRNA expression normalized against *SNRPD3* (housekeeping gene) and different letters on similar means in each cluster varies significantly ($p < 0.05$, $n = 3$) with one another and vice versa.

inhibition of NF-κB (a protein encoded by *NFkB* gene) mediate neuroprotection in neurodegenerative diseases such as Alzheimer's disease and multiple sclerosis (Srinivasan and Lahiri, 2015; Nichols et al., 2019). The present findings indicated that GMG-ITC selectively suppressed the expression of NF-kB subunits responsible for transcription of several inflammatory markers that triggers neuronal damage. On the other hand, IkBα (a protein encoded by *IkB* gene) interacted with NF-kB in two major ways namely: retention of the transcription factor (NF-kB) within cytoplasm and inhibiting its DNA binding in the nucleus, which were all enhanced due to the presence of GMG-ITC in the cells as demonstrated in Fig. 14. Studies had shown that suppression of *BACE1*-gene expression that codes for β-secretase, which is an enzyme that triggers generation of toxic fragments of the proteins was associated with neuroprotection in Alzheimer's and down syndrome disease models (Jiang et al., 2016; Zakaria and Vassar, 2018). Thus, the genotoxic effect of GMG-ITC on the expression of *BACE1* gene demonstrated the possibility of the compound to inhibit the activity of the functional BACE1 protein. Although it has beneficial effect such as regulation of synapse formation, over expression of amyloid precursor protein coded by *APP* gene was linked to increase in activity of BACE1 and concentration of amyloid beta fragments which are directly associated with pathology of AD with consequent death of neuronal cells (Kuruva and Reddy, 2017). Additionally, Tau protein encoded by *MAPT* gene is responsible for modulating axonal microtubule stability by interacting with tubulin to promote their assembly into stable form (Bodea et al., 2016). Phosphorylation of tau proteins lead to deterioration of microtubules' structure thereby generating neurofibrillary tangles that are associated with neurodegenerative disease such as AD and related tauopathies (Zhou et al., 2018).

Basically, Nrf2 is a transcription factor that translocate to nucleus when released from cytoplasm. It binds to antioxidant response element (ARE) to form complex that attaches to promoter region of phase II antioxidant genes (Velagapudi et al., 2018) and initiate expression of genes responsible for neuroprotection (Dinkova-Kostova et al., 2018). The presence of GMG-ITC therefore enhanced the expression of Nrf2 genes and its translocation to nucleus even under oxidative stress condition, which in turn affect the expression of other proteins in the pathway.

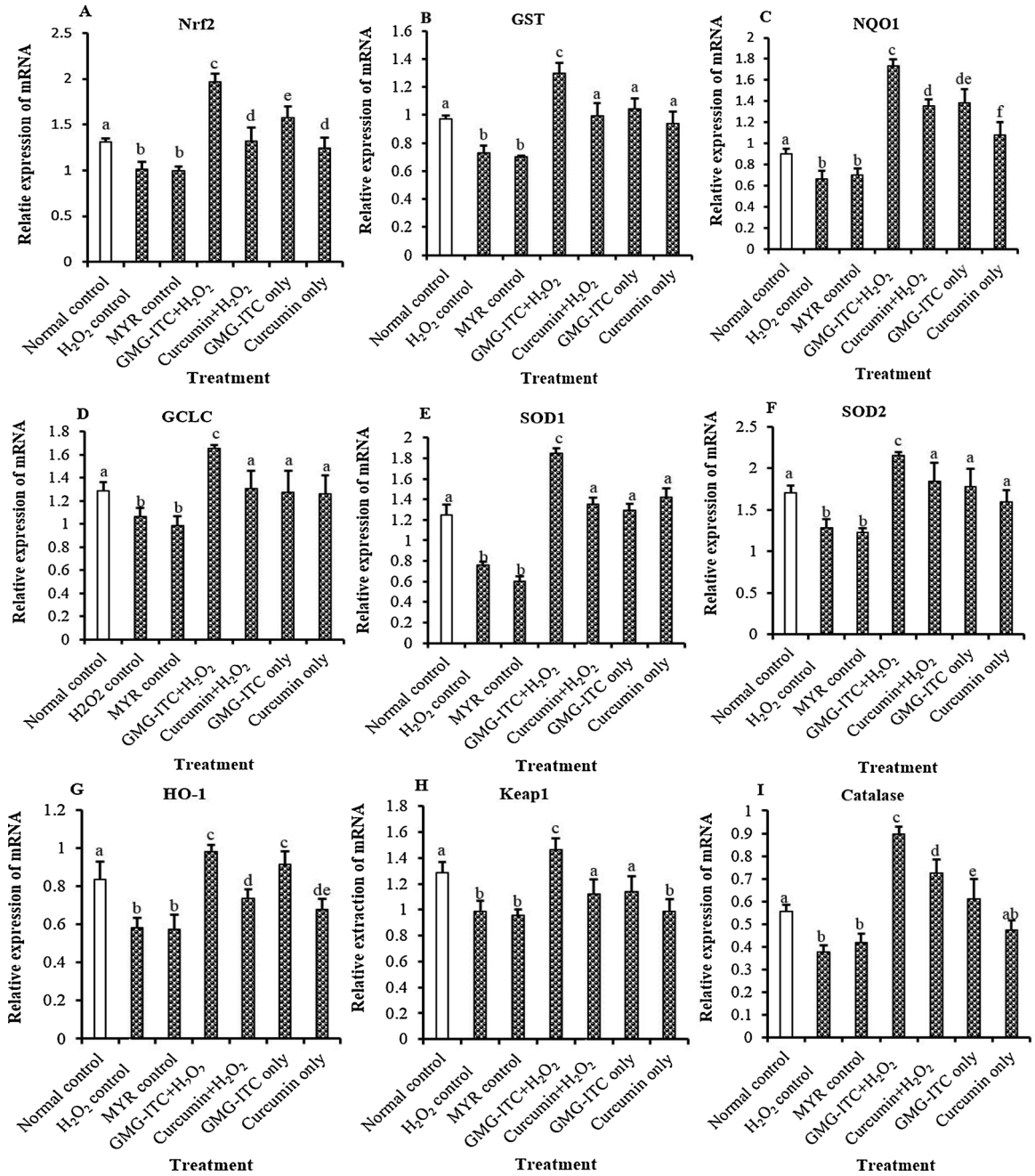

Fig. 10. Modulation of gene expression in Nrf2/ARE signalling pathway. Normal control is a group of differentiated untreated cells; H_2O_2 control: cells treated with 300 μM hydrogen peroxide only for 4 h; MYR control: myrosinase (enzyme) pre-treated and hydrogen peroxide exposed group of cells; GMG-ITC + H_2O_2: cells pre-treated with GMG-ITC for 72 h followed by 4 h exposure to H_2O_2; curcumin + H_2O_2: cells pre-treated with curcumin followed by exposure to H_2O_2 for 4 h; GMG-ITC only: and curcumin only: cells treated with only GMG-ITC and curcumin for 72 h respectively. GMG-ITC: glucomoringin isothiocyanate; H_2O_2: hydrogen peroxide. The result was expressed as relative expression of mRNA expression normalized against *SNRPD3* (housekeeping gene) and means of each cluster labelled with different letters varied significantly ($p < 0.05$, $n = 3$) with one another.

For instance, increase in expression of glutathione-*s*-transferase (GST) gene was attributed to the multiplying effect of GMG-ITC pre-treatment. GST protein play key role in neutralizing free radicals generated in the cells (Liang et al., 2018). Enhancement of GST expression by GMG-ITC indicated the ability of the compound to protect neuronal death due to oxidative damage. Also, *NQO1* gene encodes for NAD(P)H quinone dehydrogenase 1 in human, which is a pleiotropic enzyme that reduces vitamin E quinone and ubiquinone to antioxidant forms directly (Ross and Siegel, 2018). This reduction effect of quinone dehydrogenase 1 signified its primary protective role physiologically (Ross and Siegel, 2018). GMG-ITC improved the quantitative expression of NQO1 to about 1.7 folds relative to *SNRPD3* (housekeeping gene) expression. Thus, displaying possible neuroprotective activity at gene level. Our findings also showed that the multiplying effect of GMG-ITC pre-treatment caused increase in the expression of *GCLC* gene that encodes for glutamate-cysteine ligase catalytic subunit (GClc) protein, a phase II antioxidant marker with remarkable antioxidant activity in human and other related species. Level of GClc rise in response to oxidative stress and other inflammatory factors as to neutralize the environmental harmful effect and ensure protection and survival of the affected cells (Kim et al., 2015).

Interestingly, the *SOD1* and *SOD2* gene expression outcomes in the

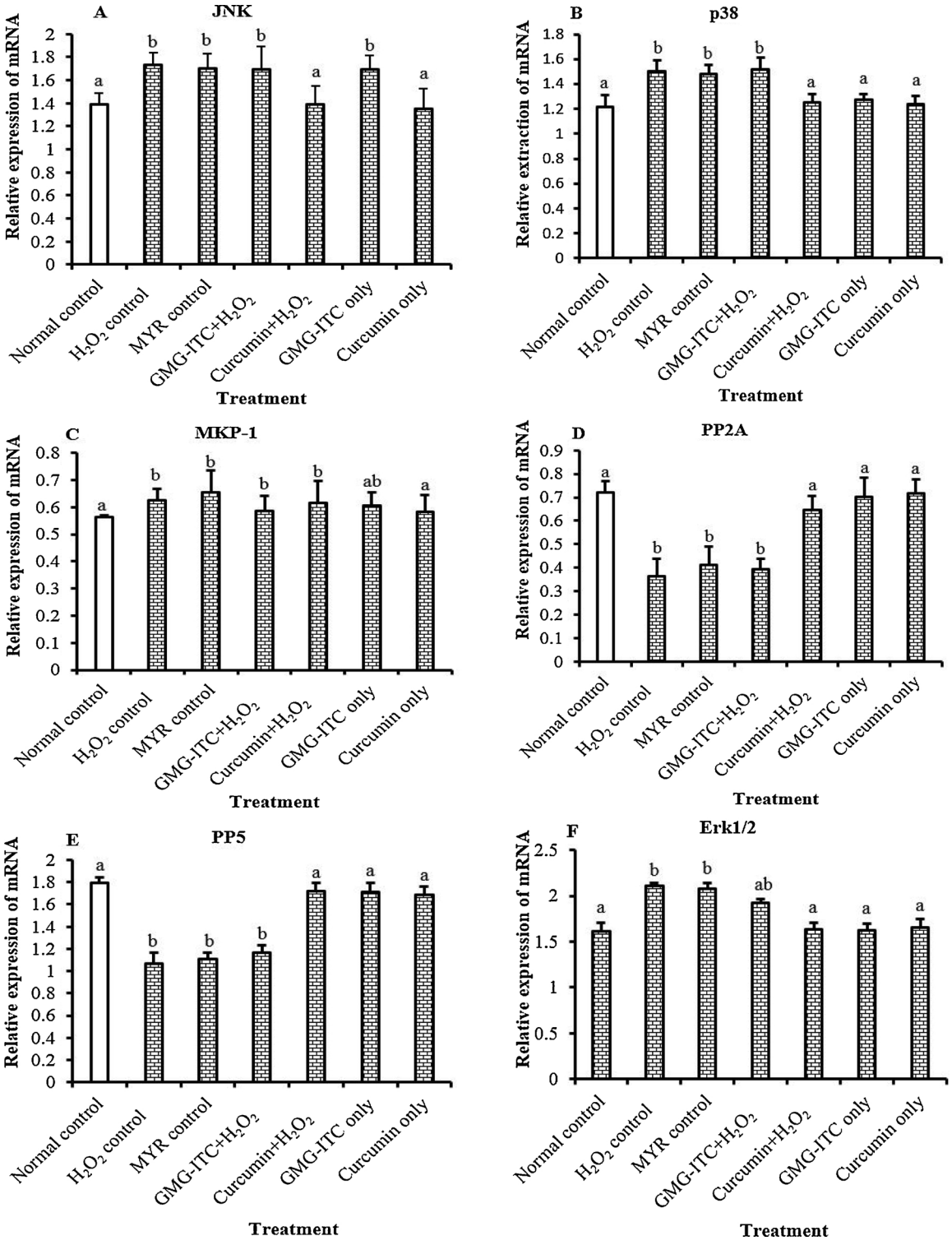

Fig. 11. Modulation of gene expression in MAPK signalling pathway. Where normal control: untreated cells; H_2O_2: cells treated with 300 μM hydrogen peroxide only for 4 h; MYR control: myrosinase (enzyme) pre-treated and hydrogen peroxide exposed group; GMG-ITC + H_2O_2: cells pre-treated with GMG-ITC for 72 h followed by 4 h exposure to hydrogen peroxide; curcumin + H_2O_2: cells pre-treated with curcumin followed by exposure to hydrogen peroxide for 4 h; GMG-ITC only: and curcumin only: cells treated with only GMG-ITC and curcumin for 72 h respectively. GMG-ITC: glucomoringin isothiocyanate, H_2O_2: hydrogen peroxide, MYR: myrosinase. The result was expressed as relative expression of mRNA expression normalized against *SNRPD3* (housekeeping gene) and different letters on similar means in each cluster varies significantly ($p < 0.05$, n = 3) with one another and vice versa.

present study followed similar trend of expression with *Nfr2* in the GMG-ITC pre-treatment group. The two genes encode for superoxide dismutase 1 and 2 enzymes, both of which are found abundantly in neural tissue. Part of the physiological and antioxidant relevance of their protein's product is regulation of superoxide concentration by dismutating the superoxide to hydrogen peroxide, a substrate to another phase II enzyme and less harmful to the former (Lalkovičová and Danielisová, 2016). This phenomenon contributes to survival of neuron

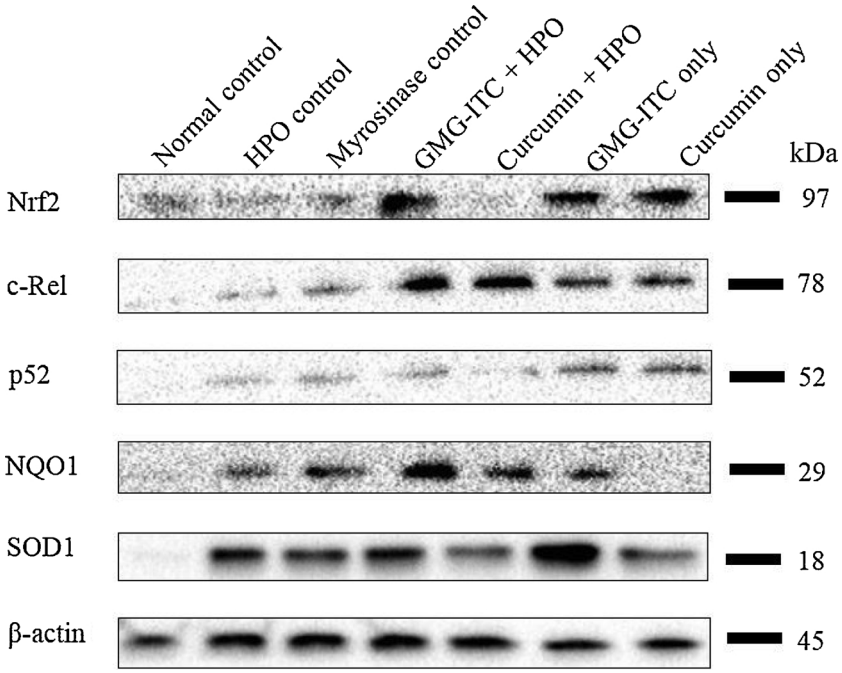

Fig. 12. Modulatory effect of GMG-ITC pre-treatment on protein translation in differentiated neuron. Nrf2, c-Rel, p52, NQO1 and SOD1 regulation was determined by immunoblotting using chemiluminescent substrates. The detected proteins were presented as bands of protein expression alongside their respected molecular weight, according to the protein ladder provided by the manufacturers. Where normal control: untreated cells; HPO: cells treated with 300 μM hydrogen peroxide only for 4 h; myrosinase control: myrosinase (enzyme) pre-treated and hydrogen peroxide exposed group; GMG-ITC + HPO: cells pre-treated with GMG-ITC for 72 h followed by 4 h exposure to hydrogen peroxide; curcumin + HPO: cells pre-treated with curcumin for 72 h followed by exposure to hydrogen peroxide for 4 h; GMG-ITC only: and curcumin only: cells treated with only GMG-ITC and curcumin for 72 h respectively. GMG-ITC: glucomoringin isothiocyanate, HPO: hydrogen peroxide.

cells in a toxic environment. Another gene that was affected by GMG-ITC pretreatment was the *HO-1* gene which is responsible for coding heme oxygenase enzyme, that catalyse the conversion of heme groups to bilirubin, a metabolite capable of scavenging free radicals such as superoxide anion, singlet oxygen and hydroxyl radicals. The enzyme was reported to provide stress tolerance and neuronal protection (Nitti et al., 2018). *Catalase* gene expression was also found to be higher in the GMG-ITC pre-treatment group due to multiplying effect of the compound. Catalase enzyme play key antioxidant role by converting harmful substances such as H_2O_2 to less toxic form (water) in the body (Dai et al., 2017). Catalase and SOD activities are fundamental detoxification processes that lead to neuronal protection and cellular longevity (Dai et al., 2017). The modulatory effect of GMG-ITC on Nrf2/ARE signalling pathway was summarized in Fig. 15, which is in line with modulatory effect of certain antioxidant agents reported previously.

Moreover, the outcomes of the present study showed that, the expression of genes for markers involved in MAPK pathway was not affected in the presence of GMG-ITC despite being in a toxic environment. *JNK* encodes for c-Jun N-terminal kinases-3 (JNK3), a neuronal specific isoform protein involved in pathology of diverse neurological disorders (Kim and Choi, 2010). Overexpression of JNK is activated by cellular stress which mediate neuronal apoptosis implicated in AD, PD and ALS (Kim and Choi, 2010; Chiu et al., 2019). Unlike the positive control, present of GMG-ITC could not prevented the genotoxic effect of H_2O_2 on the expression level of *JNK*. The *p38* gene encodes for p38 protein which is a mitogen activated protein kinase family member that play key role in MAPK pathway mediated apoptosis (Kim and Choi, 2010). The protein has been implicated in pathological processes in various tissues, such as neuronal, skeletal and cardiac tissues. Increase in activity of p38 result in excessive effect of NF-κB transcription factor (Kim and Choi, 2010). Although its expression was induced by cellular response to toxic environment, MKP-1 was reported to deactivate the MAPK families thereby reducing the inflammatory triggered via MAPK signalling pathway (Wancket et al., 2012). The authors further explained the enhancement effect of nutritional compounds and other several compounds of plant origin on MKP-1 expression (Wancket et al., 2012), which was contrary to what was observed in the present findings with respect to GMG-ITC. *PP2A* and *PP5* genes encode for two phosphatases, the major enzymes that regulate several cellular processes including growth and survival and confer neuroprotection by inhibiting ROS generation in SH-SY5Y cells and primary hippocampal neurons (Xu et al., 2018). In human, *Erk1/2* is the gene encodes for extracellular signal-regulated kinase 1 and 2 that mediate growth and development when activated in neural cells. Overexpression or high activation of this gene was implicated in pathological progression and apoptosis in neuronal cells (Li et al., 2004). The gene expression results of MAPK pathway indicated that presence of GMG-ITC did not antagonize the overexpression of inflammatory stimulated genes due to cytotoxic environment, neither enhanced the expression of phosphatases genes in MAPK signalling pathway due to oxidative stress condition. The MAPK family members (JNK, p38 and ErK½) are highly expressed in lower and higher animals (Liu et al., 2015; Xu et al., 2015). Phosphorylation of these proteins due to presence of toxicants, activates processes for cellular death such as apoptosis and or necrosis, depending on the concentration and duration of exposure to the toxicants (Wang et al., 2006; Liu et al., 2015). However, direct phosphorylation of the cytokines activated members of MAPK family by PP2A and PP5 attenuate their harmful effects of the signalling molecules (Liu et al., 2015; Shen et al., 2018). Again, due to lack of available literature on the involvement of GMG-ITC in MAPK signalling pathway gene expression, we therefore predicted that, GMG-ITC did not execute its neuroprotection activities via the pathway.

Despite the persistent arguments on genotype-phenotype relation in central dogma process, studies on protein abundance and mRNA expression level showed relative correlation between the two processes when conducted in different models (Greenbaum et al., 2003; Vogel and Marcotte, 2012; Liu et al., 2016). Suggesting that reasonable number of transcribed mRNA correlated with translation into nuclear ($r^2 = 0.8$), cell periphery ($r^2 = 0.74$) and other ($r^2 = 0.66$) proteins, despite the involvement of remarkable series of linked processes required for production and maintenance of cellular proteins from transcripts (Vogel and Marcotte, 2012; Liu et al., 2016). As such, we assume most of the expressed mRNA in the present study translated in to protein, since they are majorly nuclear and cytoplasmic proteins.

It was learned previously that, NF-kB transcription factor that includes RelA (p65), RelB, p50, c-Rel, and p52 exist in two forms as dimers namely constitutive and inducible factors in which their functions vary in the neuronal cells (Baldwin, 1996; Mattson and Meffert, 2006). The physiological functions of constitutive form of NF-kB subunits has

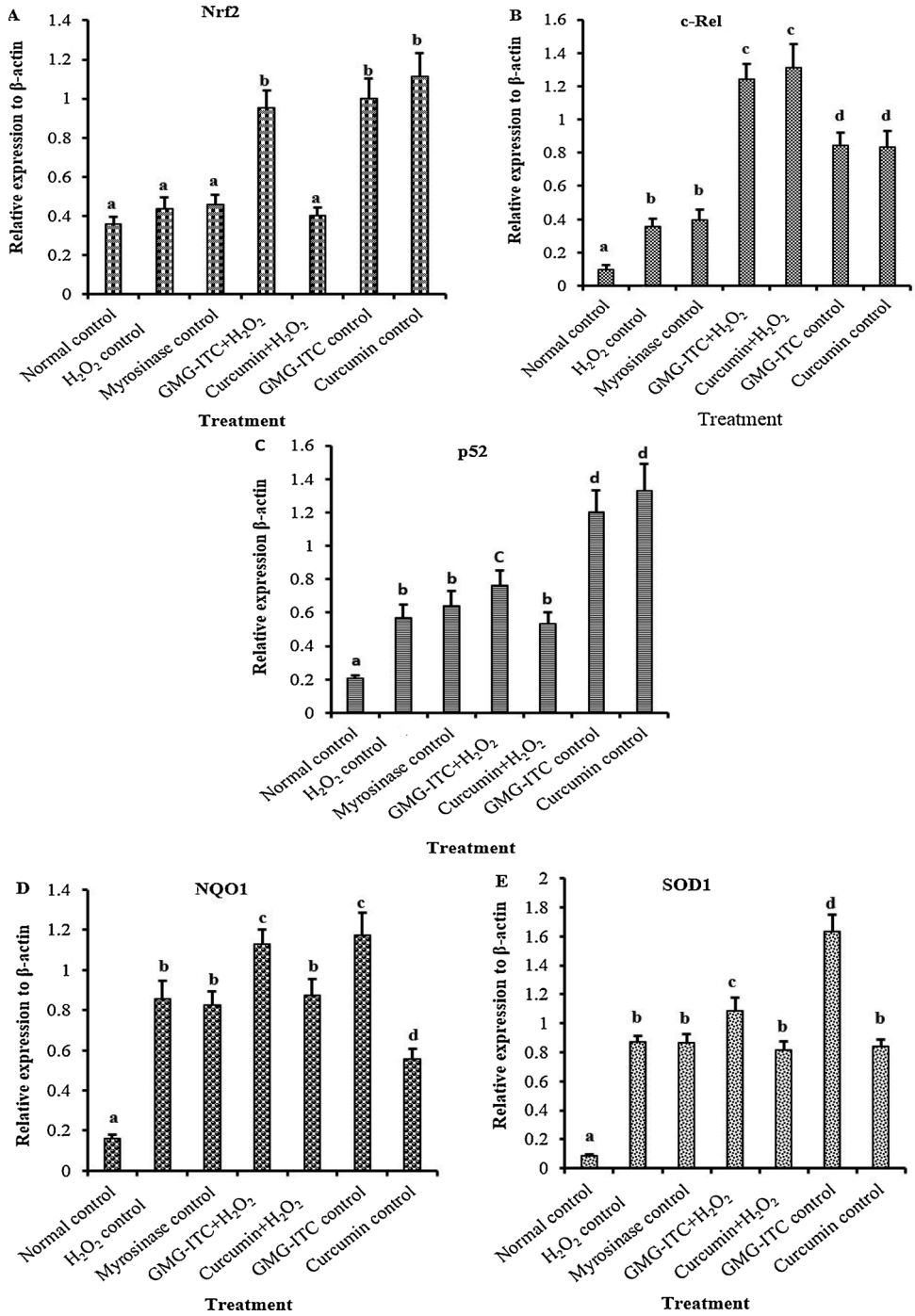

Fig. 13. Modulatory effect of GMG-ITC pre-treatment on Nrf2, c-Rel, p52, NQO1 and SOD1 protein expression. The expressed proteins were presented as relative intensity of protein expression in folds normalized against β-actin. H_2O_2, hydrogen peroxide; values are expressed as mean of relative expression of proteins normalised against β-actin (housekeeping protein). Means with different letters differed significantly (ANOVA, $p < 0.05$) with one another at 95 confidence level.

been linked with long term memory formation, synaptic plasticity formation, survival of neurons, growth and development of dendrites at moderate expression (Smale, 2011), while the inducible form of NF-kB marker is critical for responses adapted for neuronal degeneration after exposure to certain level of toxic stimuli in noxious environment (Sarnico et al., 2009; Gupta et al., 2010). Therefore, GMG-ITC was suggested to have modulated the expression of proteins that are directly involved in its neuroprotective activity through Nrf2/ARE and NF-kB/IkB pathways.

5. Conclusions

The findings of the present study highlighted the implication of GMG-ITC in the expression of genes and key proteins that mediate signal transductions in NF-kB/IkB, Nrf2 and MAPK signalling pathways. The effect seemed to slow down the expression and translocation of p65 and p50 dimer transcription factor into nucleus. However, the compound upregulated the expression of transcription factors (c-ReL and p52) involved in constitutive signalling of NF-kB pathway which enhance the protection and survival of cell in a toxic environment. Unlike the putative influence of the compound on internal defense mechanism

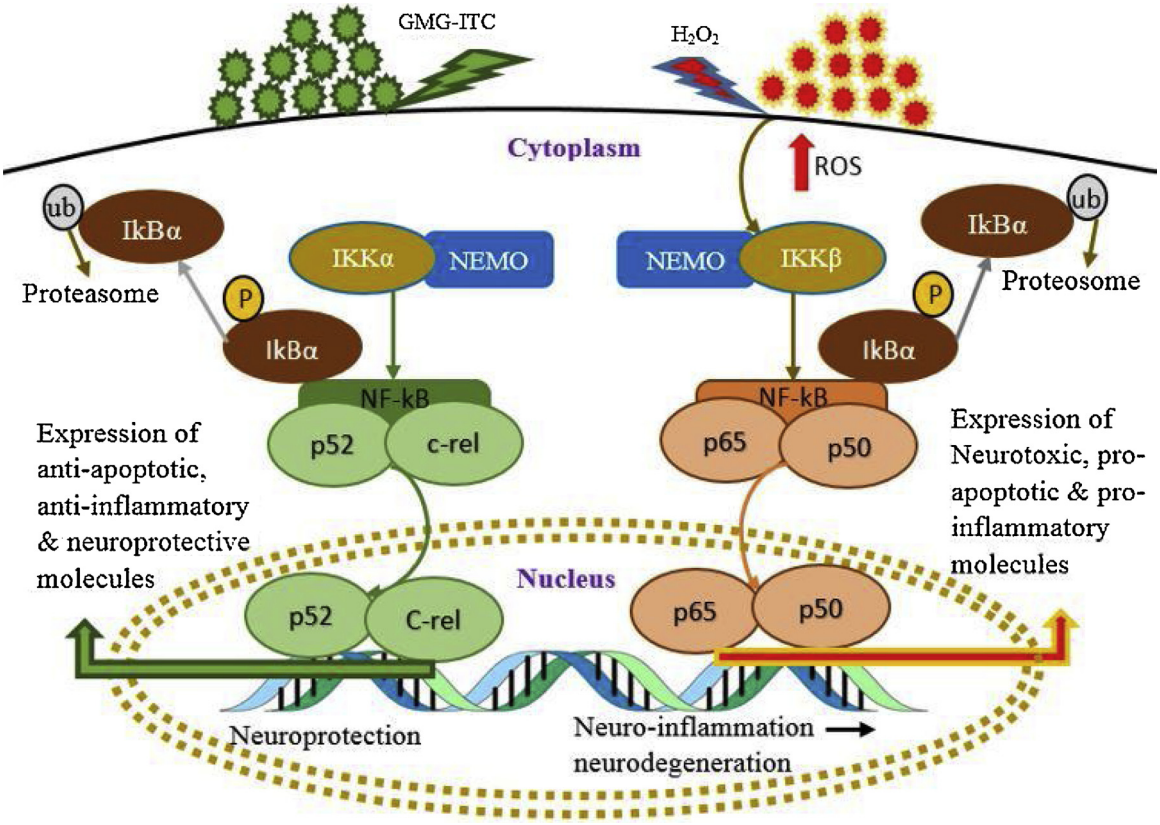

Fig. 14. Predicted neuroprotective effect of GMG-ITC via NF-kB signalling pathway. IKK: IkB kinase; NEMO: NF-kB essential modulator; ROS: Reactive oxygen species.

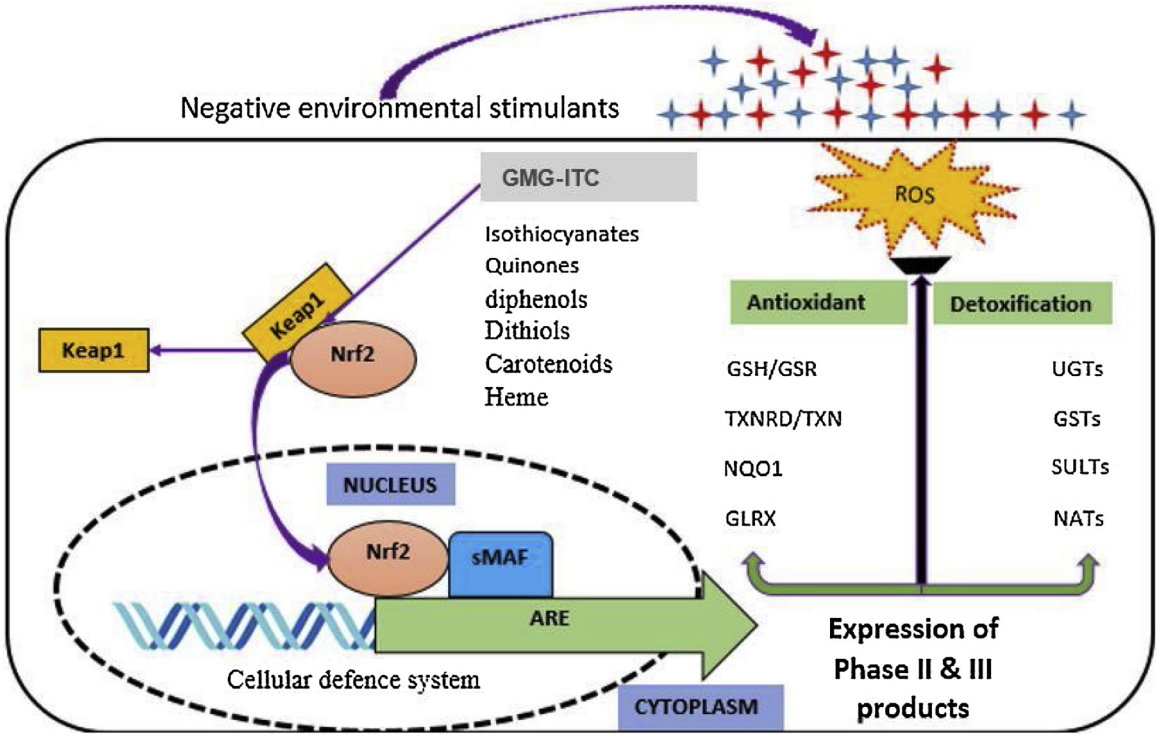

Fig. 15. Predicted neuroprotective effect of GMG-ITC via Nrf2/ARE signalling pathway. Here various inducers caused the release of cytoplasmic Nrf2 from its anchored molecule (Keap1) and localised to nucleus to form transcription complex. ARE: Antioxidant response element; Glrx: Glutaredoxin; GSH: Glutathione; GSR: Glutathione-disulfide reductase; GSTs: Glutathione *S*-transferases; Keap1: Kelch-like ECH-associated protein 1; NATs: N-acetyltransferases; Nrf2: Nuclear factor erythroid 2-related factor 2; NQO1: NAD(P)H quinone dehydrogenase 1; ROS: Reactive oxygen species; sMAF: proto-oncogene response element; SULTs: Sulfotransferases; TXN: Thioredoxin; TXNRD: Thioredoxin reductase; UGTs: UDP glucuronosyltransferases.

system of cells through Nrf2 pathway reported above, GMG-ITC did not seem to affect the expression of genes involved in MAPK signalling pathway. This finding revealed the potential of GMG-ITC in diminution of oxidative stress damage via NF-kB/IkB and enhanced neuronal protection and survival through Nrf2/ARE signalling pathways. This is perhaps the first study to discover and suggest new pathway related to neuroprotective activity of GMG-ITC.

Author contributions

MSJ, NN, KS, RR and AFAR: conceived and designed the experiments; MSJ, NN, and AFAR: performed the experiments and analyzed the data; MSJ, HYB, NN, NMN and AFAR: drafted and proofread the paper; all authors read and approved the final manuscript.

Funding

This work was funded by Universiti Putra Malaysia through GP-IPS (Vot no. 9537300) and GP (Vot no. 9628600).

Declaration of Competing Interest

The authors declared that there is no conflict of interest.

Acknowledgments

Our appreciation goes to MitoMasa Sdn. Bhd., Malaysia, for the provision of *Moringa oleifera* seeds sample used in this study. We thank Dr. Leon Sze Wei for his guide in the isolation part of this study. We also appreciate the effort and support from Dr. Ooi Der Jiun and Dr. Norsharina Ismail throughout the study period.

References

Abdull, R., Ahmad, F., Ibrahim, M.D., Kntayya, S.B., 2014. Health benefits of moringa oleifera. Asian Pac. J. Cancer Prev. 15 (20), 8571–8576.

Al-Asmari, A.K., Albalawi, S.M., Athar, M.T., Khan, A.Q., Al-Shahrani, H., Islam, M., 2015. Moringa oleifera as an anti-cancer agent against breast and colorectal cancer cell lines. PLoS One 10 (8), e0135814.

Baldwin Jr, A.S., 1996. The NF-κB and IκB proteins: new discoveries and insights. Annu. Rev. Immunol. 14 (1), 649–681.

Baxter, L.C., Sparks, D.L., Johnson, S.C., Lenoski, B., Lopez, J.E., Connor, D.J., Sabbagh, M.N., 2006. Relationship of cognitive measures and gray and white matter in Alzheimer's disease. J. Alzheimer Dis. 9 (3), 253–260.

Bodea, L.G., Eckert, A., Ittner, L.M., Piguet, O., Götz, J., 2016. Tau physiology and pathomechanisms in frontotemporal lobar degeneration. J. Neurochem. 138, 71–94.

Brettschneider, J., Del Tredici, K., Lee, V.M.Y., Trojanowski, J.Q., 2015. Spreading of pathology in neurodegenerative diseases: a focus on human studies. Nat. Rev. Neurosci. 16 (2), 109.

Chen, H., Kwong, J.C., Copes, R., Tu, K., Villeneuve, P.J., Van Donkelaar, A., Hystad, P., Martin, R.V., Murray, B.J., Jessiman, B., Wilton, A.S., 2017. Living near major roads and the incidence of dementia, Parkinson's disease, and multiple sclerosis: a population-based cohort study. Lancet 389 (10070), 718–726.

Chen, L., Liu, L., Yin, J., Luo, Y., Huang, S., 2009. Hydrogen peroxide-induced neuronal apoptosis is associated with inhibition of protein phosphatase 2A and 5, leading to activation of MAPK pathway. Int. J. Biochem. Cell Biol. 41 (6), 1284–1295.

Cheung, Y.T., Lau, W.K.W., Yu, M.S., Lai, C.S.W., Yeung, S.C., So, K.F., Chang, R.C.C., 2009. Effects of all-trans-retinoic acid on human SH-SY5Y neuroblastoma as in vitro model in neurotoxicity research. Neurotoxicology 30 (1), 127–135.

Chiu, Y.J., Hsieh, Y.H., Lin, T.H., Lee, G.C., Hsieh-Li, H.M., Sun, Y.C., Chen, C.M., Chang, K.H., Lee-Chen, G.J., 2019. Novel compound VB-037 inhibits Aβ aggregation and promotes neurite outgrowth through enhancement of HSP27 and reduction of P38 and JNK-mediated inflammation in cell models for Alzheimer's disease. Neurochem. Int. 125, 175–186.

Dai, D.F., Chiao, Y.A., Martin, G.M., Marcinek, D.J., Basisty, N., Quarles, E.K., Rabinovitch, P.S., 2017. Mitochondrial-targeted catalase: extended longevity and the roles in various disease models. Prog. Mol. Biol. Transl. Sci. 146, 203–241 Academic Press.

De Graaf, R.M., Krosse, S., Swolfs, A.E., Te Brinke, E., Prill, N., Leimu, R., Van Galen, P.M., Wang, Y., Aarts, M.G., Van Dam, N.M., 2015. Isolation and identification of 4-α-rhamnosyloxy benzyl glucosinolate in noccaea caerulescens showing intraspecific variation. Phytochemistry 110, 166–171. https://doi.org/10.1016/j.phytochem.2014.11.016.

Dinkova-Kostova, A.T., Kostov, R.V., Kazantsev, A.G., 2018. The role of Nrf2 signaling in counteracting neurodegenerative diseases. FEBS J. 285 (19), 3576–3590.

Ferguson, R., Subramanian, V., 2016. PA6 stromal cell co-culture enhances SH-SY5Y and VSC4. 1 neuroblastoma differentiation to mature phenotypes. PLoS One 11 (7), e0159051.

Galuppo, M., Giacoppo, S., De Nicola, G.R., Iori, R., Navarra, M., Lombardo, G.E., Bramanti, P., Mazzon, E., 2014. Antiinflammatory activity of glucomoringin isothiocyanate in a mouse model of experimental autoimmune encephalomyelitis. Fitoterapia 95, 160–174.

Galuppo, M., Nicola, G., Iori, R., Dell'Utri, P., Bramanti, P., Mazzon, E., 2013. Antibacterial activity of glucomoringin bioactivated with myrosinase against two important pathogens affecting the health of long-term patients in hospitals. Molecules 18 (11), 14340–14348.

Galuppo, M., Giacoppo, S., Iori, R., De Nicola, G.R., Milardi, D., Bramanti, P., Mazzon, E., 2015a. 4 (α-L-rhamnosyloxy)-benzyl isothiocyanate, a bioactive phytochemical that defends cerebral tissue and prevents severe damage induced by focal ischemia/reperfusion. J. Biol. Regul. Homeost. Agents 29, 343–356.

Galuppo, M., Giacoppo, S., Iori, R., De Nicola, G.R., Bramanti, P., Mazzon, E., 2015b. Administration of 4-(α-L-rhamnosyloxy)-benzyl isothiocyanate delays disease phenotype in SOD1G93A rats: a transgenic model of amyotrophic lateral sclerosis. Biomed. Res. Int. 2015.

Giacoppo, S., Galuppo, M., De Nicola, G.R., Iori, R., Bramanti, P., Mazzon, E., 2015. 4(α-l-rhamnosyloxy)-benzyl isothiocyanate, a bioactive phytochemical that attenuates secondary damage in an experimental model of spinal cord injury. Bioorg. Med. Chem. 23 (1), 80–88.

Greenbaum, D., Colangelo, C., Williams, K., Gerstein, M., 2003. Comparing protein abundance and mRNA expression levels on a genomic scale. Genome Biol. 4 (9), 117.

Gupta, S.C., Sundaram, C., Reuter, S., Aggarwal, B.B., 2010. Inhibiting NF-κB activation by small molecules as a therapeutic strategy. Biochimic. Biophys. Acta Gene Regul. Mech. 1799 (10), 775–787.

Ismail, N., Ismail, M., Imam, M.U., Azmi, N.H., Fathy, S.F., Foo, J.B., Bakar, M.F.A., 2014. Mechanistic basis for protection of differentiated SH-SY5Y cells by oryzanol-rich fraction against hydrogen peroxide-induced neurotoxicity. BMC Complement. Altern. Med. 14 (1), 467. https://doi.org/10.1186/1472-6882-14-467.

Ismail, N., Ismail, M., Azmi, N.H., Bakar, A., Firdaus, M., Basri, H., Abdullah, M.A., 2016. Modulation of hydrogen peroxide-induced oxidative stress in human neuronal cells by thymoquinone-rich fraction and thymoquinone via transcriptomic regulation of antioxidant and apoptotic signaling genes. Oxid. Med. Cell. Longev. 2016.

Jaafaru, M.S., Kyomson, I.D., Waziri, P.M., Yakubu, Y., Mustapha, M.B., Gyutorwa, J.S., 2017. In vivo ameliorative effect of methanolic extract of boswellia dalzielli Hutch (Mebdh) stem bark on Triton X-100 induced hyperlipidaemia. Sci. World J. 12 (4), 34–37.

Jaafaru, M., Abd Karim, N., Mohamed Eliaser, E., Maitalata Waziri, P., Ahmed, H., Mustapha Barau, M., Kong, L., Abdull Razis, A., 2018a. Nontoxic glucomoringin-isothiocyanate (GMG-ITC) rich soluble extract induces apoptosis and inhibits proliferation of human prostate adenocarcinoma cells (PC-3). Nutrients 10 (9), 1174.

Jaafaru, M., Abd Karim, N., Enas, M., Rollin, P., Mazzon, E., Abdull Razis, A., 2018b. Protective effect of glucosinolates hydrolytic products in neurodegenerative diseases (NDDs). Nutrients 10 (5), 580.

Jaafaru, M.S., Nordin, N., Shaari, K., Rosli, R., Razis, A.F.A., 2018c. Isothiocyanate from moringa oleifera seeds mitigates hydrogen peroxide-induced cytotoxicity and preserved morphological features of human neuronal cells. PLoS One 13 (5), e0196403. https://doi.org/10.1371/journal.pone.0196403.

Jaja-Chimedza, A., Graf, B.L., Simmler, C., Kim, Y., Kuhn, P., Pauli, G.F., Raskin, I., 2017. Biochemical characterization and anti-inflammatory properties of an isothiocyanate-enriched moringa (moringa oleifera) seed extract. PLoS One 12 (8), e0182658. https://doi.org/10.1371/journal.pone.0182658.

Jiang, Y., Rigoglioso, A., Peterhoff, C.M., Pawlik, M., Sato, Y., Bleiwas, C., Stavrides, P., Smiley, J.F., Ginsberg, S.D., Mathews, P.M., Levy, E., 2016. Partial BACE1 reduction in a Down syndrome mouse model blocks Alzheimer-related endosomal anomalies and cholinergic neurodegeneration: role of APP-CTF. Neurobiol. Aging 39, 90–98.

Karim, N.A.A., Ibrahim, M.D., Kntayya, S.B., Rukayadi, Y., Hamid, H.A., Razis, A.F.A., 2016. Moringa oleifera Lam: targeting chemoprevention. Asian Pac. J. Cancer Prev. 17, 3675–3686.

Kim, D.W., Lee, K.T., Kwon, J., Lee, H.J., Lee, D., Mar, W., 2015. Neuroprotection against 6-OHDA-induced oxidative stress and apoptosis in SH-SY5Y cells by 5, 7-dihydroxychromone: activation of the Nrf2/ARE pathway. Life Sci. 130, 25–30.

Kim, E.K., Choi, E.J., 2010. Pathological roles of MAPK signalling pathways in human diseases. Biochimic. Biophys. Acta Mol. Basis Dis. 1802 (4), 396–405.

Kim, J., Kim, S.K., Kim, H.K., Mattson, M.P., Hyun, D.H., 2013. Mitochondrial function in human neuroblastoma cells is up-regulated and protected by NQO1, a plasma membrane redox enzyme. PLoS One 8 (7), e69030.

Korecka, J.A., van Kesteren, R.E., Blaas, E., Spitzer, S.O., Kamstra, J.H., Smit, A.B., Swaab, D.F., Verhaagen, J., Bossers, K., 2013. Phenotypic characterization of retinoic acid differentiated SH-SY5Y cells by transcriptional profiling. PLoS One 8 (5), e63862.

Kovacs, G.G., 2016. Molecular pathological classification of neurodegenerative diseases: turning towards precision medicine. Int. J. Mol. Sci. 17 (2), 189.

Kumar, A., Singh, A., 2015. A review on Alzheimer's disease pathophysiology and its management: an update. Pharmacol. Rep. 67 (2), 195–203.

Kumssa, D.B., Joy, E.J., Young, S.D., Odee, D.W., Ander, E.L., Broadley, M.R., 2017. Variation in the mineral element concentration of moringa oleifera Lam. and M. stenopetala (Bak. f.) Cuf.: role in human nutrition. PLoS One 12 (4), e0175503. https://doi.org/10.1371/journal.pone.0175503.

Kuruva, C.S., Reddy, P.H., 2017. Amyloid beta modulators and neuroprotection in Alzheimer's disease: a critical appraisal. Drug Discov. Today 22 (2), 223–233.

Lalkovičová, M., Danielisová, V., 2016. Neuroprotection and antioxidants. Neural Regener. Res. 11 (6), 865.

Li, Z., Arnaud, L., Rockwell, P., Figueiredo-Pereira, M.E., 2004. A single amino acid

substitution in a proteasome subunit triggers aggregation of ubiquitinated proteins in stressed neuronal cells. J. Neurochem. 90 (1), 19–28.
Liang, D., Gao, F., Ni, Z., Lin, L., Deng, Q., Tang, Y., Wang, X., Luo, X., Xia, H., 2018. Melatonin improves heat tolerance in kiwifruit seedlings through promoting antioxidant enzymatic activity and glutathione S-transferase transcription. Molecules 23 (3), 584.
Liu, C., Zhang, R., Sun, C., Zhang, H., Xu, C., Liu, W., Gao, W., Huang, S., Chen, L., 2015. Resveratrol prevents cadmium activation of Erk1/2 and JNK pathways from neuronal cell death via protein phosphatases 2A and 5. J. Neurochem. 135 (3), 466–478.
Liu, Y., Beyer, A., Aebersold, R., 2016. On the dependency of cellular protein levels on mRNA abundance. Cell 165 (3), 535–550.
Mangieri, L.R., Mader, B.J., Thomas, C.E., Taylor, C.A., Luker, A.M., Tonia, E.T., Huisingh, C., Shacka, J.J., 2014. ATP6V0C knockdown in neuroblastoma cells alters autophagy-lysosome pathway function and metabolism of proteins that accumulate in neurodegenerative disease. PLoS One 9 (4), e93257.
Mastrantonio, R., Cervelli, M., Pietropaoli, S., Mariottini, P., Colasanti, M., Persichini, T., 2016. HIV-Tat induces the Nrf2/ARE pathway through NMDA receptor-elicited spermine oxidase activation in human neuroblastoma cells. PLoS One 11 (2), e0149802.
Mattson, M.P., Meffert, M.K., 2006. Roles for NF-κB in nerve cell survival, plasticity, and disease. Cell Death Differ. 13 (5), 852.
Michl, C., Vivarelli, F., Weigl, J., De Nicola, G.R., Canistro, D., Paolini, M., Iori, R., Rascle, A., 2016. The chemopreventive phytochemical moringin isolated from moringa oleifera seeds inhibits JAK/STAT signaling. PLoS One 11 (6) p.e0157430.
Nichols, M.R., St-Pierre, M.K., Wendeln, A.C., Makoni, N.J., Gouwens, L.K., Garrad, E.C., Sohrabi, M., Neher, J.J., Tremblay, M.E., Combs, C.K., 2019. Inflammatory mechanisms in neurodegeneration. J. Neurochem. 149 (5), 562–581.
Nitti, M., Piras, S., Brondolo, L., Marinari, U., Pronzato, M., Furfaro, A., 2018. Heme oxygenase 1 in the nervous system: does it favor neuronal cell survival or induce neurodegeneration? Int. J. Mol. Sci. 19 (8), 2260.
Park, H.R., Lee, H., Park, H., Jeon, J.W., Cho, W.K., Ma, J.Y., 2015. Neuroprotective effects of Liriope platyphylla extract against hydrogen peroxide-induced cytotoxicity in human neuroblastoma SH-SY5Y cells. BMC Complement Altern. Med. 15 (1), 171.
Raina, R., Sen, D., 2018. Can crosstalk between DOR and PARP reduce oxidative stress mediated neurodegeneration? Neurochem. Int. 112, 206–218.
Rajan, T.S., Giacoppo, S., Iori, R., De Nicola, G.R., Grassi, G., Pollastro, F., Bramanti, P., Mazzon, E., 2016. Anti-inflammatory and antioxidant effects of a combination of cannabidiol and moringin in LPS-stimulated macrophages. Fitoterapia 112, 104–115.
Razis, A.F.A., Bagatta, M., De Nicola, G.R., Iori, R., Ioannides, C., 2011. Induction of epoxide hydrolase and glucuronosyl transferase by isothiocyanates and intact glucosinolates in precision-cut rat liver slices: importance of side-chain substituent and chirality. Arch. Toxicol. 85 (8), 919–927.
Richards, C.E., Vellanki, S.H., Smith, Y.E., Hopkins, A.M., 2018. Diterpenoid natural compound C4 (Crassin) exerts cytostatic effects on triple-negative breast cancer cells via a pathway involving reactive oxygen species. Cell. Oncol. 41 (1), 35–46.
Ross, D., Siegel, D., 2018. NQO1 in protection against oxidative stress. Curr. Opin. Toxicol. 7, 67–72.
Sahin, S., Önal, T.O., Cinar, N., Bozdemir, M., Çubuk, R., Karsidag, S., 2017. Distinguishing depressive pseudodementia from alzheimer disease: a comparative study of hippocampal volumetry and cognitive tests. Dement. Geriatr. Cogn. Dis. Extra 7 (2), 230–239.
Santana-Gómez, C.E., Valle-Dorado, M.G., Domínguez-Valentín, A.E., Hernández-Moreno, A., Orozco-Suárez, S., Rocha, L., 2018. Neuroprotective effects of levetiracetam, both alone and combined with propylparaben, in the long-term consequences induced by lithium-pilocarpine status epilepticus. Neurochem. Int. 120, 224–232.
Sarnico, I., Lanzillotta, A., Benarese, M., Alghisi, M., Baiguera, C., Battistin, L., Spano, P., Pizzi, M., 2009. NF-kappaB dimers in the regulation of neuronal survival. Int. Rev. Neurobiol. 85, 351–362.
Sharma, D., Barhwal, K.K., Biswal, S.N., Srivastava, A.K., Bhardwaj, P., Kumar, A., Chaurasia, O.P., Hota, S.K., 2018. Hypoxia-mediated alteration in cholesterol oxidation and raft dynamics regulates BDNF signalling and neurodegeneration in hippocampus. J. Neurochem.
Shen, T., Zhu, W., Dou, L., Gu, H., Zhang, L., Chen, H., Zhou, Q., Sanchez, E.R., Field, L., Mayo, L.D., Xie, Z., 2018. Protein phosphatase 5 and the tumor suppressor P53 downregulate each other's activities in mice. J. Biol. Chem. 293 (47), 18218–18229 jbc-RA118.
Singh, D., Reeta, K.H., Sharma, U., Jagannathan, N.R., Dinda, A.K., Gupta, Y.K., 2019. Neuro-protective effect of monomethyl fumarate on ischemia reperfusion injury in rats: role of Nrf2/HO1 pathway in peri-infarct region. Neurochem. Int. 126, 96–108.
Smale, S.T., 2011. Hierarchies of NF-κB target-gene regulation. Nat. Immunol. 12 (8), 689.
Solanki, I., Parihar, P., Parihar, M.S., 2016. Neurodegenerative diseases: from available treatments to prospective herbal therapy. Neurochem. Int. 95, 100–108.
Srinivasan, M., Lahiri, D.K., 2015. Significance of NF-κB as a pivotal therapeutic target in the neurodegenerative pathologies of Alzheimer's disease and multiple sclerosis. Expert Opin. Ther. Targets 19 (4), 471–487.
Toffa, D.H., Magnerou, M.A., Kassab, A., Djibo, F.H., Sow, A.D., 2019. Can magnesium reduce central neurodegeneration in Alzheimer's disease? Basic evidences and research needs. Neurochem. Int. 126, 195–202.
Velagapudi, R., El-Bakoush, A., Olajide, O.A., 2018. Activation of Nrf2 pathway contributes to neuroprotection by the dietary flavonoid tiliroside. Mol. Neurobiol. 1–21.
Vogel, C., Marcotte, E.M., 2012. Insights into the regulation of protein abundance from proteomic and transcriptomic analyses. Nat. Rev. Genet. 13 (4), 227.
Wancket, L.M., Frazier, W.J., Liu, Y., 2012. Mitogen-activated protein kinase phosphatase (MKP)-1 in immunology, physiology, and disease. Life Sci. 90 (7–8), 237–248.
Wang, Z., Yang, H., Tachado, S.D., Capó-Aponte, J.E., Bildin, V.N., Koziel, H., Reinach, P.S., 2006. Phosphatase-mediated crosstalk control of ERK and p38 MAPK signaling in corneal epithelial cells. Invest. Ophthalmol. Visual Sci. 47 (12), 5267–5275.
Waziri, P.M., Abdullah, R., Rosli, R., Omar, A.R., Abdul, A.B., Kassim, N.K., Malami, I., Etti, I.C., Sani, J.A.M., Lila, M.A.M., Abdullah, J.F.F., 2018. Clausenidin induces caspase 8-Dependent apoptosis and suppresses production of VEGF in liver Cancer cells. Asian Pac. J. Cancer Prev. 19 (4), 917.
Xu, C., Zhang, H., Liu, C., Zhu, Y., Wang, X., Gao, W., Huang, S., Chen, L., 2015. Rapamycin inhibits Erk1/2-mediated neuronal apoptosis caused by cadmium. Oncotarget 6 (25), 21452.
Xu, Z., Chen, S., Wang, Y., Chen, S., Yao, W., Gao, X., 2018. Neuroprotective effects of silk fibroin hydrolysate against Aβ 25–35 induced cytotoxicity in SH-SY5Y cells and primary hippocampal neurons by regulating ROS inactivation of PP2A. J. Funct. Foods 45, 100–109.
Zakaria, J.A.D., Vassar, R.J., 2018. A promising, novel, and unique BACE1 inhibitor emerges in the quest to prevent Alzheimer's disease. EMBO Mol. Med. 10 (11), e9717.
Zhou, L., Yao, G.D., Lu, L.W., Song, X.Y., Lin, B., Wang, X.B., Huang, X.X., Song, S.J., 2018. Neolignans from red raspberry (Rubus idaeus L.) exhibit enantioselective neuroprotective effects against H2O2-induced oxidative injury in SH-SY5Y cells. J. Agric. Food Chem. 66 (43), 11390–11397.